

## 7. SITES 875/876<sup>1</sup>

### Shipboard Scientific Party<sup>2</sup>

#### HOLE 875A

**Date occupied:** 15 June 1992  
**Date departed:** 16 June 1992  
**Time on hole:** 1 hr, 15 min  
**Position:** 12°00.756'N, 164°56.466'E  
**Bottom felt (rig floor; m, drill-pipe measurement):** 1422.0  
**Distance between rig floor and sea level (m):** 11.2  
**Water depth (drill-pipe measurement from sea level, m):** 1410.8  
**Total depth (rig floor; m):** 1433.2  
**Penetration (m):** 11.2  
**Number of cores (including cores with no recovery):** 1  
**Total length of cored section (m):** 11.20  
**Total core recovered (m):** 0.25  
**Core recovery (%):** 2.2  
**Oldest sediment cored:**  
Depth (mbsf): 11.2  
Nature: carbonate sand  
Age: Maastrichtian

#### HOLE 875B

**Date occupied:** 16 June 1992  
**Date departed:** 16 June 1992  
**Time on hole:** 4 hr, 45 min  
**Position:** 12°06.156'N, 164°56.466'E  
**Bottom felt (rig floor; m, drill-pipe measurement):** 1421.0  
**Distance between rig floor and sea level (m):** 11.2  
**Water depth (drill-pipe measurement from sea level, m):** 1409.8  
**Total depth (rig floor; m):** 1461.0  
**Penetration (m):** 40.0  
**Number of cores (including cores with no recovery):** 4  
**Total length of cored section (m):** 40.00  
**Total core recovered (m):** 1.95  
**Core recovery (%):** 4.9  
**Oldest sediment cored:**  
Depth (mbsf): 40.0  
Nature: skeletal packstone-limestone  
Age: Maastrichtian

#### HOLE 875C

**Date occupied:** 16 June 1992  
**Date departed:** 17 June 1992

**Time on hole:** 21 hr, 45 min  
**Position:** 12°00.756'N, 164°56.466'E  
**Bottom felt (rig floor; m, drill-pipe measurement):** 1420.0  
**Distance between rig floor and sea level (m):** 11.2  
**Water depth (drill-pipe measurement from sea level, m):** 1408.8  
**Total depth (rig floor; m):** 1553.0  
**Penetration (m):** 133.0  
**Number of cores (including cores with no recovery):** 15  
**Total length of cored section (m):** 133.0  
**Total core recovered (m):** 17.62  
**Core recovery (%):** 13.2  
**Oldest sediment cored:**  
Depth (mbsf): 126.0  
Nature: packstone and grainstone-limestone  
Age: mid-Maastrichtian to Campanian  
Measured velocity (km/s): 3.7–4.3  
**Hard rock:**  
Depth (mbsf): 126.6  
Nature: basalt  
**Basement:**  
Depth (mbsf): 126.6  
Nature: basalt

#### HOLE 876A

**Date occupied:** 17 June 1992  
**Date departed:** 19 June 1992  
**Time on hole:** 21 hr, 30 min  
**Position:** 12°14.796'N, 164°55.908'E  
**Bottom felt (rig floor; m, drill-pipe measurement):** 1410.0  
**Distance between rig floor and sea level (m):** 11.2  
**Water depth (drill-pipe measurement from sea level, m):** 1398.8  
**Total depth (rig floor; m):** 1564.0  
**Penetration (m):** 154.0  
**Number of cores (including cores with no recovery):** 17  
**Total length of cored section (m):** 154.0  
**Total core recovered (m):** 14.82  
**Core recovery (%):** 9.6  
**Oldest sediment cored:**  
Depth (mbsf): 139.5  
Nature: grainstone, packstone, limestone  
Age: Maastrichtian to Campanian  
**Hard rock:**  
Depth (mbsf): 145.0  
Nature: basalt  
**Basement:**  
Depth (mbsf): 145.0  
Nature: basalt  
Measured velocity (km/s): 4.3–4.6

**Principal results:** Sites 875 and 876 are located on the northeastern rim of Wodejebato Guyot (formerly Sylvania Guyot), in the Ralik Chain of the

<sup>1</sup> Premoli Silva, I., Haggerty, J., Rack, F., et al., 1993. *Proc. ODP, Init. Repts.*, 144: College Station, TX (Ocean Drilling Program).

<sup>2</sup> Shipboard Scientific Party is as given in the list of participants preceding the contents.

northern Marshall Islands. Sites 875/876 are situated 1.67 km apart, atop a discontinuous outer perimeter ridge; this ridge is persistent along the north and east margin rim of the guyot. The outer perimeter ridge appears as a constructional feature in the seismic profiles.

Coring began at Site 875 on 16 June 1992 and was completed on 17 June after 1.6 days. After obtaining our drilling objectives in Hole 875C and retrieving the beacon, we departed Site 875 on 17 June 1992 and moved on to Site 876. Coring began at Site 876 on 18 June 1992 and was completed on 19 June after 0.9 days.

Site 875 is located at 12°00.72'N, 164°56.44'E in a water depth of 1409 m, and Site 876 is located at 12°01.47'N, 164°55.90'E in a water depth of 1399 m. The sites are positioned along the seaward crest of the outer perimeter ridge. Objectives at these sites were (1) to determine the composition and origin of the outer perimeter ridge; (2) to determine its relationship to the evolution of the guyot; (3) to investigate the variability of the outer perimeter ridge; (4) to establish the characteristics of the facies and facies changes with time; (5) to examine the diagenesis of the limestones; (6) to determine the nature of the acoustic basement reflector beneath the outer perimeter ridge; and (7) to evaluate the vertical tectonic history of the platform relative to sea level.

Three holes were drilled at Site 875 and one hole was drilled at Site 876. Before spudding in Hole 875A using the rotary coring bit (RCB), a seafloor survey was conducted using the vibration-isolated television (VIT). The relatively flat sandy area had 1-m high outcrops coated with manganese crust. The first 11-m core from Hole 875A had a recovered of 25 cm of poorly cemented, coarse skeletal sands of Maastrichtian age. Hole 875A immediately showed indications of caving and was abandoned. After another videotape (VIT) survey, Hole 875B was spudded in 10 m northwest of Hole 875A and was cored with the RCB as a bare-rock spud-in. After coring 40 m of coarse, poorly cemented skeletal sand (4.9% recovery), Hole 875B was abandoned because of poor hole conditions. About 16 m north-northwest from Hole 875A, Hole 875C was successfully drilled as a bare rock spud-in, using a DCB-Geoset bit, and cored to 133 msbf total depth (TD). Recovery in Hole 875C averaged 13.2%.

No VIT survey was conducted before spudding in Hole 876A because the 3.5-kHz echo-sounder profiles indicated a thin pelagic sediment cover. Hole 876A was rotary cored using an anti-whorl polycrystalline-diamond-compact (PDC) bit to 154 msbf (TD). The average recovery was 9.6%. Poor hole conditions prevented our logging in Holes 875C and 876A.

Three lithologic units were recognized at Sites 875 and 876 using a combination of visual core descriptions and smear slide and thin-section data. The age of these units was based on the identification of larger benthic foraminifers and macrofossils (rudists), and calcareous nannofossils and planktonic foraminifers. The units, as recognized from top to bottom, are described as follows:

Unit I (0–0.14 msbf, Hole 875C; 0–0.08 msbf, Hole 876A) consists of an upper middle Eocene foraminifer limestone, penetrated by manganese-oxide dendrites, that overlies a manganese encrusted, phosphatized, Maastrichtian skeletal packstone. The packstone contains cavities filled in with phosphatized pelagic sediments of late middle Eocene, early Eocene, and late Paleocene age. In Hole 876A, the packstone matrix contains lower Eocene pelagic sediment that has filtered into the limestone.

Unit II (0–0.36 msbf, Hole 875A; 0–30.83 msbf, Hole 875B; 0.14–126 msbf, Hole 875C; 0.08–145.5 msbf, Hole 876A) consists of skeletal grainstone and packstone of middle to possibly late Maastrichtian age. The average carbonate content is 99%. White to pale brown, lightly cemented, solution-etched, coarse-grained skeletal grainstone contains abundant larger foraminifers (*Sulcoperculina* and *Asterorbis*), red algae (corallineaceans and squamariaceans), and rudist debris (mainly radiolitids with few caprinids). Planktonic foraminifers are few to rare widely disseminated. Minor components are corals, green algae (dasycladaceans), echinoderms, and bryozoans. Unit II has been divided into three subunits. The middle subunit is composed of skeletal packstone with lenses of wackestone. The porosity is intergranular and moldic. Average grainstone porosity is 28% to 40%; porosity in the packstone is about 10%. A few small basalt fragments are incorporated at the bottom of Unit II. A filled cavity at least 30 cm in length extends into the upper surface of Unit II at Site 876. The

former cavity is lined by manganese oxide and filled in with planktonic foraminifer limestone of middle Eocene age.

Unit III (126–133 msbf, Hole 875C; 145.5–154.0 msbf, Hole 876A) consists of highly vesicular basalt, possibly alkali olivine basalt, with 1% to 2% pyrite in the uppermost part of the unit in Hole 875C. In Hole 876A, highly altered alkali basalt and intercalated volcanic breccia were recovered. Three massive basalt flow units, each less than a few meters thick, and one basaltic breccia were identified from Hole 876A. The uppermost basalt flows are brownish in color and appear to have undergone a relatively brief period of oxidative weathering. The volcanic breccia is composed of subangular to subrounded basalt fragments that are similar in texture to that of the underlying alkali basalt flow; this suggests that the breccia formed as the top of the lava flow. Magnetic measurements were undertaken on a few discrete samples of basalt and breccia from Sites 875 and 876. The range of inclination of all the samples is from +2° to +30°, compatible with a reversed magnetization acquired in a low southern latitude.

## BACKGROUND AND OBJECTIVES

For a discussion of the geologic history of Wodejebato Guyot and previous studies, see the "Background and Objectives" section of the Site 873 chapter (this volume).

Sites 875 and 876 are located on the northeastern rim of Wodejebato Guyot in the northern Marshall Islands. These two sites are atop the outer perimeter ridge; they are separated by 1.67 km along the seaward crest of this ridge.

The drilling strategy at Wodejebato Guyot evolved on the basis of the results obtained at Sites 873 and 874. The skeletal limestone recovered at Site 874, from the inner perimeter ridge, raised questions about the composition and origin of the nearly parallel outer perimeter ridge. The age and development of this feature is an important factor in determining the evolution of Wodejebato Guyot. The outer perimeter ridge appears as a constructional feature in the seismic profiles.

The specific objectives at Sites 875 and 876 were (1) to investigate the nature and variability of the outer perimeter ridge, (2) to establish the characteristics of the facies and changes with time, (3) to examine the diagenesis of the limestones, and (4) to evaluate the vertical tectonic history of the atoll relative to sea level.

Drilling at Sites 875 and 876 was successful. The primary objectives associated with these sites are addressed with the preliminary shipboard studies and additional shore-based studies.

## OPERATIONS

### Site 875, Wodejebato Guyot, Outer Perimeter Ridge

The study of Maastrichtian platform limestone at Site 874, on the inner perimeter ridge, raised questions about the composition and origin of the parallel outer perimeter ridge that rims the northeastern side of Wodejebato Guyot. From the seismic profiles, the ridge appears to be a constructional feature. The age and development of this feature is an important factor for determining the evolution of Wodejebato Guyot. A location approximately 0.5 nmi to the north of Site 874 was chosen for the drill site. The move was accomplished in dynamic positioning (DP) mode after the Site 874 beacons were recovered and while the drill-string round trip was in progress.

#### Hole 875A

A new RCB bottom-hole assembly (BHA) was assembled with a MBR because logging was a possibility, and the drill string was deployed. The VIT was run for a seafloor survey to find a favorable location. The relatively flat sandy area had 1-m high outcrops coated with a manganese crust. After about 1.25 hr of surveying

in the outcrop region, a rock-rimmed depression was found that was about 1.2 m deep and 1.5 m wide and floored with a thin sediment accumulation. The bit was set into the "natural reentry cone," and the drill string was compensated while the VIT was recovered.

Hole 875A was spudded-in at 0415L (L= local time) 16 June 1992 in a water depth of 1411 m. The first core was expected to be drilled slowly because a highly cemented limestone was anticipated. Surprisingly, the first core of 11 m was drilled in 13 min. The core barrel recovered 25 cm of coarse, poorly cemented skeletal grainstone. The hole showed indications of caving and did not yield the anticipated indurated limestone; the hole was abandoned in the hope that the debris was a localized occurrence.

#### Hole 875B

Another VIT reconnaissance was conducted, and a second (slightly broader) sediment-filled depression was located about 10 m northwest of Hole 875A in an area of hummocky outcrops. Pump circulation was attempted before the VIT was recovered to determine whether the floor of the depression was soft enough to "jet away." The seafloor held 6,000 to 8,000 lb of weight on the bit (WOB) despite the jetting action, and the VIT was pulled for the spud-in.

Rotation began and again the bit had the same rapid rate of penetration (ROP). Recovery was 36 cm of the Maastrichtian skeletal limestone. Coring then proceeded with the anticipation that reef rock could be found beneath a veneer of carbonate-sand debris. After drilling Core 144-875B-4R to 40 mbsf with no change in results and an average core recovery of 4.9%, the hole seemed to collapse and the drill string became temporarily stuck during retrieval of the core. The hole was abandoned because of poor hole conditions and low core recovery.

#### Hole 875C

We decided to retrieve the pipe and to change from the rotary system to a diamond core barrel (DCB) system that used a Geoset bit in an effort to improve recovery in the poorly cemented skeletal grainstone. In addition, the irregular, low-relief (0.5 m) seafloor was considered acceptable for a bare-rock spud-in without any further VIT surveying. The spud was considered preferable to compensating the string with unsupported weight on the weak drill-collar connections while the VIT was retrieved. Maximum ship's heave at the time was about 1 m. The videotape record showed an appropriate seafloor topography for several meters in all directions, with the most favorable just to the west; therefore, a 10-ft offset was requested during the pipe trip.

When preparations for spudding were made, the pipe was lowered to "tag" the seafloor to determine water depth. Surprisingly, firm seafloor was found about 2 m higher than at the previous hole; this difference was greater than the total relief observed during the survey. As the tag had potentially hit the highest rock in the area, a slight offset of 10 ft south was requested. The subsequent tag found that the seafloor was about 0.5 m deeper, and the bit was lowered for the spud. We learned later that a miscommunication between the rig floor and DP control had resulted in a west offset of 10 m instead of 10 ft. Hole 875C was in a water depth of 1409 m and 16 m north-northwest from Hole 875A.

The spud was accomplished with minimum rotation speed (40 rpm) and just enough WOB to keep the bit from lifting off the bottom. Maximum ship's heave was about 1 m. The first meter required 18 min to penetrate; the ROP increased slightly with depth and 63 min elapsed before the core was cut. The core barrel could not be retrieved until several meters were drilled, to avoid pulling above the seafloor and having to respud. When the barrel eventually was recovered, a piece of manganese crust with "spin"

marks on its lower surface was found at the top of the core, indicating that it was jammed in the throat of the bit, taking much of the limited bit weight away from the cutting structure. Apparently, this piece of manganese crust was forced into the core barrel after most of the interval had been cored; about 50 cm of limestone lay beneath the crust.

Coring then continued in poorly cemented skeletal grainstone and rudstone, resulting in increasing ROP and decreasing core recovery. Hole-cleaning problems began after Core 144-875C-4M, and the pipe became firmly stuck while the barrel of Core 144-875C-5M was being retrieved, despite the use of mud sweeps. Apparently, unconsolidated carbonate sand had collapsed around the drill collars and filled the narrow ( $7\frac{1}{4} \times 6\frac{3}{4}$  in.) annulus. After about 45 min, the string was worked free with an overpull of 120,000 lb and high torque. Additional mud sweeps were successful in cleaning the hole, and coring resumed. A similar, but less serious, sticking incident occurred in Core 144-875C-13M, but again the hole restabilized with mud sweeps.

No further hole trouble was encountered. The DCB system required some adjustments as personnel learned to work with the combination of a small annulus, low circulation rates, and light bit weight; otherwise the system posed no operational problems.

Table 1. Coring summary, Sites 875 and 876.

Core no.	Date (June 1992)	Time (Z)	Depth (mbsf)	Cored (m)	Recovered (m)	Recovery (%)
144-875A-1R	15	1815	0-11.2	11.2	0.25	2.2
Coring totals				11.2	0.25	2.2
144-875B-1R	15	2130	0-11.2	11.2	0.36	3.2
2R	15	2235	11.2-20.7	9.5	0.28	3.0
3R	15	2340	20.7-30.3	9.6	0.95	9.9
4R	16	0045	30.3-40.0	9.7	0.36	3.7
Coring totals				40.0	1.95	4.9
144-875C-1M	16	1115	0-9.5	9.5	0.60	6.3
2M	16	1215	9.5-17.5	8.0	1.10	13.7
3M	16	1325	17.5-27.1	9.6	0.66	6.9
4M	16	1425	27.1-36.8	9.7	0.61	6.3
5M	16	1610	36.8-46.4	9.6	1.22	12.7
6M	16	1720	46.4-56.0	9.6	1.07	11.1
7M	16	1815	56.0-65.7	9.7	0.68	7.0
8M	16	1915	65.7-75.3	9.6	0.39	4.1
9M	16	2035	75.3-85.0	9.7	0.50	5.2
10M	16	2140	85.0-94.7	9.7	2.46	25.3
11M	16	2250	94.7-104.3	9.6	3.30	34.4
12M	17	0020	10.3-113.9	9.6	1.50	15.6
13M	17	0155	11.9-123.6	9.7	2.16	22.2
14M	17	0315	12.6-126.6	3.0	0.67	22.3
15M	17	0700	12.6-133.0	6.4	0.69	10.8
16B	17	1100	0-133.0	133.0	0.01	0
Coring totals				266.0	17.62	6.6
144-876A-1R	17	1820	0-14.2	14.2	0.62	4.4
2R	17	1920	14.2-23.7	9.5	0.32	3.4
3R	17	2015	23.7-33.3	9.6	0.65	6.8
4R	17	2105	33.3-43.0	9.7	0.98	10.1
5R	17	2200	43.0-52.6	9.6	2.31	
6R	17	2340	52.6-62.2	9.6	0.04	0.4
7R	18	0040	62.2-71.9	9.7	1.22	12.6
8R	18	0130	71.9-81.5	9.6	1.10	11.4
9R	18	0215	81.5-91.2	9.7	0.37	3.8
10R	18	0320	91.2-100.8	9.6	0.40	4.2
11R	18	0445	100.8-110.5	9.7	1.92	19.8
12R	18	0545	110.5-120.1	9.6	0.28	2.9
13R	18	0645	120.1-129.8	9.7	1.30	13.4
14R	18	0750	129.8-139.4	9.6	0.80	8.3
15R	18	0930	139.4-147.8	8.4	0.68	8.1
16R	18	1200	147.8-150.0	2.2	0.78	35.8
17R	18	1435	150.0-154.0	4.0	1.00	25.0
18B	18	2000	0-154.0	154.0	0.05	0
Coring totals				308.0	14.82	4.8

Average core recovery in these poorly cemented limestones was 13.2%, but this was still more than double the recovery obtained using the RCB system in similar material in Holes 875A and 875B (see Table 1).

At 126.3 mbsf, the bit contacted basalt. Highly altered and fractured basalts were cored from 126.3 to 133 mbsf; both cores became jammed. Drilling ended at 133 mbsf (TD), and the drill string was recovered. The positioning beacon was recovered after the bit cleared the seafloor, and the DP/GPS move to Site 876 began while the pipe trip was in progress.

Overall, performance of the DCB Geoset bit in the basalt was roughly equivalent to the RCB, but the DCB bit was not designed for drilling igneous rock. Upon recovery, the DCB bit was found to have severe damage to its cutting structure; most of the diamond cutters were sheared off or broken and about three-fourths of the cutting structure was gone. Had the bit not been pulled and had we continued to drill, the outer one-third of the face of the bit would have worn out prematurely in comparison to the other cutting surfaces on the bit.

### Site 876—Wodejebato Guyot, Outer Perimeter Ridge

The morphology of the outer ridge appeared similar to the parallel inner perimeter ridge, which contained some reef facies, but the limestone recovered from Site 875 was reef debris. An additional site was chosen to determine the variability of the facies in the outer perimeter ridge. The ship was moved in DP mode 1.67 km northwest along the axis of the ridge and 10 m higher in elevation. Bathymetry and sediment cover were monitored using the record from the 3.5-kHz echo sounder while the move was in progress. The beacon was launched at 2245L 17 June 1992.

#### Hole 876A

An additional effort was made to improve recovery and to evaluate alternative coring hardware; the RCB BHA was fitted with a drag-type "anti-whirl" polycrystalline-diamond-compact (PDC) bit. No VIT survey was conducted before spudding Hole 876A because the 3.5-kHz records indicated about 4 m of pelagic cover. This thin pelagic sediment cover was expected to provide enough lateral resistance to prevent the bit from "skating" on the hard manganese-encrusted phosphatized hardground.

Before the spud was attempted, the bit was lowered to tag the seafloor and to determine its depth. The weight indicator and motion compensator began to react when the bit reached 1410 m below the driller's datum, or 1399 m below sea level (mbsl). The bit then was lowered with slow rotation and no circulation in an attempt to "punch-core" the expected watery foraminifer ooze above the hardground. Hard resistance was met at 3 mbsf; minimal weight and circulation were applied to begin coring the limestone. Little penetration was seen for a few minutes, but then an increase in torque signaled that the PDC cutters had begun to bite into the hardground. After a hard 1 m, the bit broke through into much softer material, and only 22 min were required to core the initial 14.2-m interval. The hole was "over-drilled" by a few meters to ensure that a connection could be made without pulling out of the hole.

Upon recovery, the first core contained none of the soft pelagic material, but the manganese crust and associated phosphatized hardground were recovered. Below the hardground was some poorly cemented grainstone; total recovery was 62 cm.

As coring continued, hole-cleaning problems again appeared at about 40–50 mbsf, and it was necessary to spend about 30 min freeing the pipe and cleaning the hole after Core 144-876A-5R. As before, the hole stabilized and no further hole troubles were encountered. Core recovery in the poorly cemented grainstone

was somewhat lower than with the DCB, but a 3-m-thick bed of packstone that was not well represented at Site 875 was recovered at Site 876.

Basalt was contacted at 145 mbsf and was cored to total depth (TD) at 154 mbsf. Bit performance was essentially equivalent to that of the other coring systems, but the condition of the highly altered and fractured basalt made it a poor standard of comparison. Core 144-876A-16R was pulled early because low ROP and torque indicated possible bit failure. Instead, the problem was a core jam. The ROP increased upon resumption of coring, but recovery of the final core was only 25%. Using the anti-whorl PDC, average recovery was only 9.6%, with a range of 35.4% to <1% (see Table 1).

About 25,000 lb of drag was noted as the drill string was tripped out of the hole. Hole 876A was not logged because of the questionable stability of the hole; the heave of the ship producing drill-pipe movement in the hole could have enhanced the instability of the hole and endangered the logging tools.

Upon recovery of the string, the bit showed considerable wear to the cutting structure, with the diamond cutting edge chipped away on the majority of the PDCs. One jet nozzle was missing and one was plugged with claylike material, a drilling artifact from the altered basalt.

## LITHOSTRATIGRAPHY

### Lithologic Units

The outer perimeter ridge of northeastern Wodejebato Guyot was cored at Sites 875 and 876 on the ridge crest. The correlative sedimentary rocks recovered from these sites are the easiest to characterize and among the most difficult to interpret of any site drilled on Wodejebato Guyot.

Each of three holes at Site 875 and a single hole at Site 876 was spudded directly into manganese-encrusted limestone; no cover of unconsolidated sediment was encountered. Three tries were required at Site 875 to core through the 126 m of limestone into the basalt. One core was recovered from Hole 875A before the hole was lost. Hole 875B yielded 1.95 m of limestone in four cores. At Hole 875C, 16.8 m of skeletal grainstone were recovered, which represented 13.3% recovery from the limestone sequence. At Site 876, located 1.6 km north-northwest of Site 875 on presumed depositional strike, basaltic basement was reached without misadventure. Recovery from the 145.5-m limestone interval totaled 11.63 m or 8%.

Three correlative lithologic units are recognized from the two sites (Figs. 1–3 and Table 2).

#### Unit I

Nature: manganese-encrusted, planktonic foraminifer limestone  
 Intervals: Hole 875C, Core 144-875C-1M; Hole 876A, Core 144-876A-1R  
 Depth: Hole 875C, 0–0.14 mbsf; Hole 876A, 0–0.08 mbsf  
 Age: late Paleocene through late middle Eocene

Two samples of manganese crust and planktonic-foraminifer limestone were recovered in Hole 875C. The two crust samples are quite different (Figs. 4–5), so they may represent two distinct crusts, although the ages of the associated limestones overlap. A single crust was recovered at Site 876. No crusts were recovered at Holes 875A and 875B. The VIT surveys of the seafloor during hole location indicate that the entire surface is manganese encrusted; thus, the absence of crust at Holes 875A and 875B appears to be from poor recovery.

The upper crust (Interval 144-875C-1M, 0–7 cm; Interval 144-876A-1R, 0–8 cm) appears dense, structureless, and black (N2); it is 1–3 cm thick. On a favorably fractured surface, three

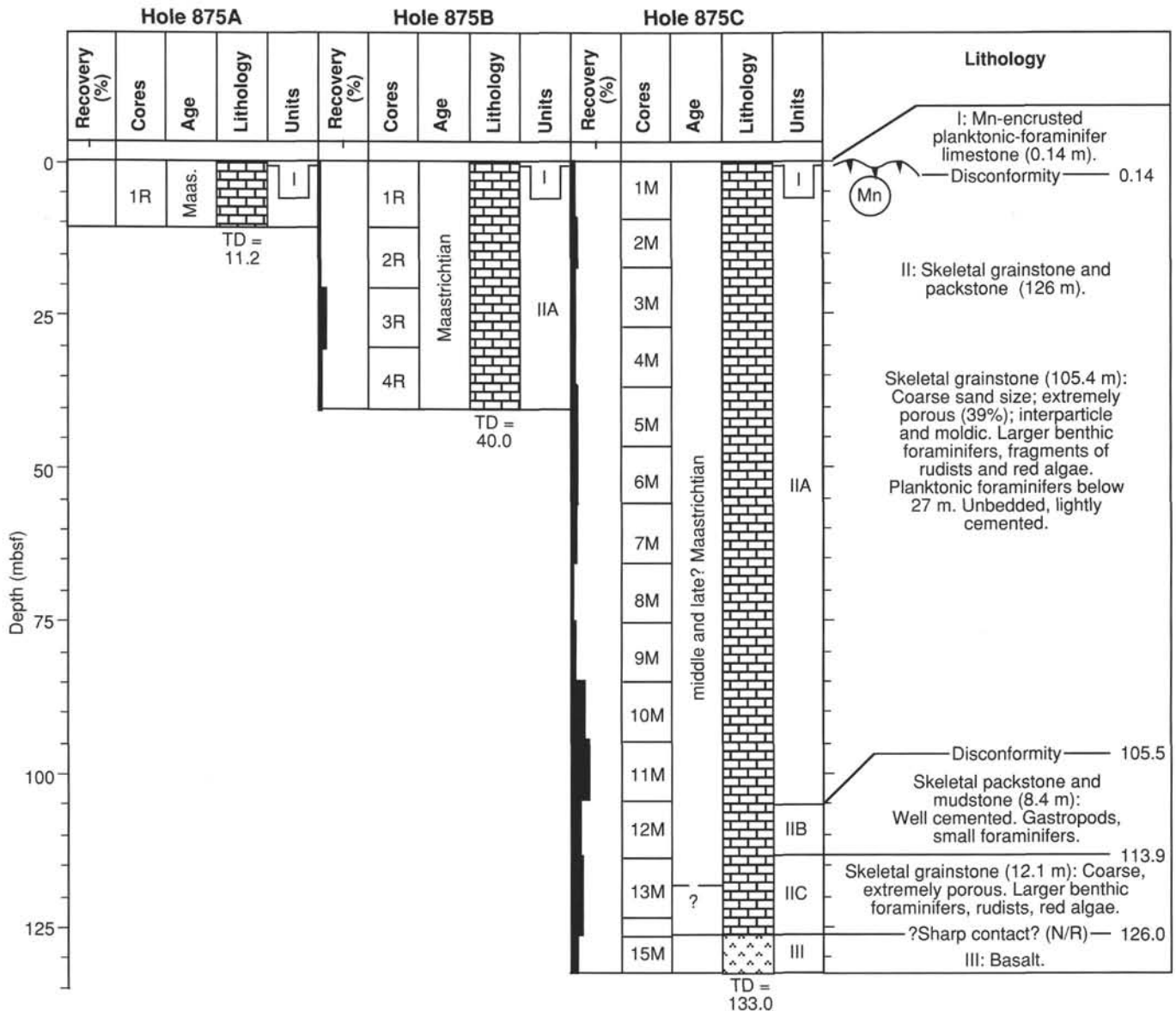


Figure 1. Lithostratigraphic summary of Site 875.

laminated intervals, 1–2 mm thick, alternate with two digitate layers 1.5 and 5 mm thick. The digits are botryoidal, formed by stacks of submillimeter hemispheres. The total thickness of the five layers is about one-third of the recovered crust; many such layers may exist within the crust.

Each crust recovered in Hole 875C is overlain by foraminifer limestone that is variously shaded white (10YR 8/2), gray (10YR 7/3), and very pale brown (10YR 7/4). The limestone, which has a packstone texture, contains abundant and varied planktonic foraminifers in a matrix of lime mud and nanofossils. Ages determined from the microfossils are late Paleocene through late middle Eocene (see “Biostratigraphy” section, this chapter). Dendrites of manganese extend upward into the foraminifer limestone, impregnating matrix and fossils seemingly at random. The dendritic pattern is particularly striking in Interval 144-875C-1M, 7–14 cm; it resembles a series of columnar stromatolites separated by pelagic limestone (Fig. 5), just as the individual digits resemble very elongate, stacked hemispheroids on a much smaller scale. Color variation within the pelagic limestone probably reflects the

degree of impregnation by phosphate, the other bane of condensed pelagic sections.

### Unit II

Nature: skeletal grainstone and packstone

Intervals: Hole 875A, Core 144-875A-1R; Hole 875B, Cores 144-875B-1R through -4R; Hole 875C, Sections 144-875C-1M-1, 14 cm, to -14M-1, 65 cm; Hole 876A, Sections 144-876A-1R-1, 8 cm, to -15R-1, 12 cm

Depth: Hole 875C, 0.14–126 mbsf; Hole 876A, 0.08–145.5 mbsf

Age: middle and late? Maastrichtian, possibly Campanian at base

Unit II includes the entire limestone succession between the manganese crust and basalt at Sites 875 and 876. It is essentially a pile of lightly cemented, solution-etched, coarse-grained skeletal grainstone. The unit is punctuated at about 100 mbsf by a well-cemented interval of slightly muddy skeletal sand that includes a thin mudstone layer in Hole 875C. This contrasting interval necessitates subdividing the skeletal limestones into three subunits, of which the upper and lower are similar grainstones.

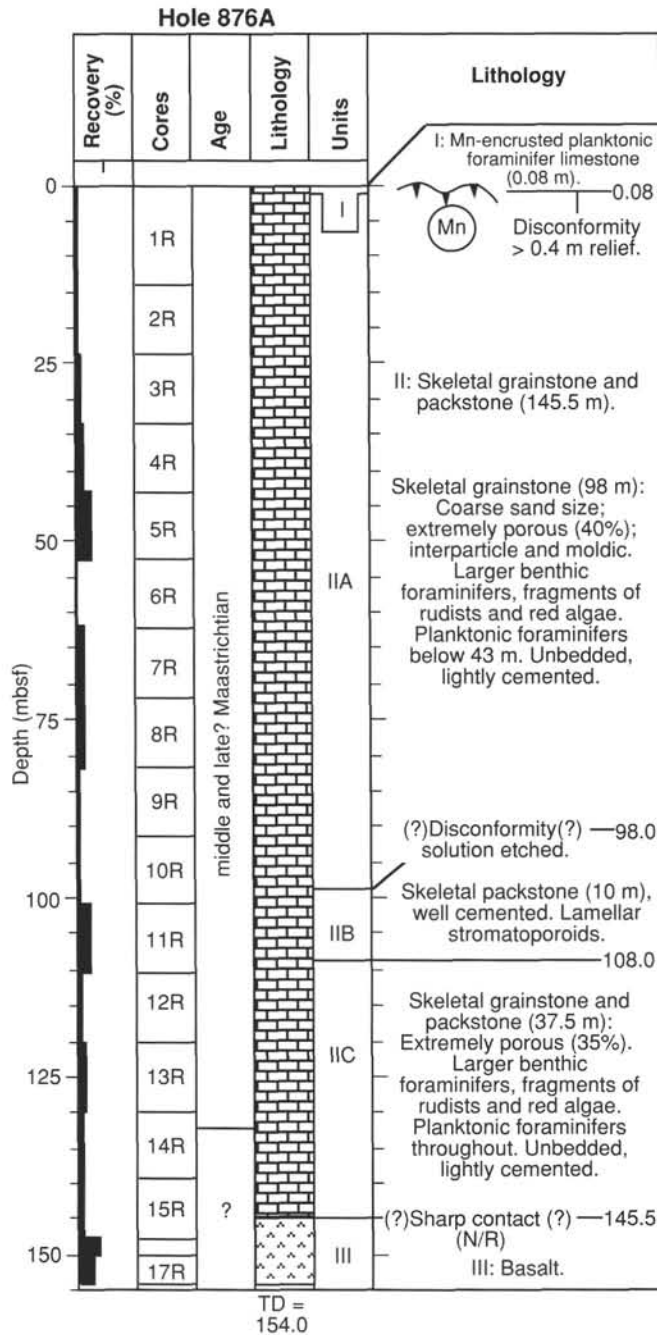


Figure 2. Lithostratigraphic summary of Site 876.

### Subunit IIA

Nature: porous skeletal grainstone

Intervals: Hole 875A, Core 144-875A-1R; Hole 875B, Cores 144-875B-1R through -4R; Hole 875C, Sections 144-875C-1M-1, 14 cm, to -12M-1, 125 cm; Hole 876A, Section 144-876A-1R-1, 8 cm, through Core 144-876A-9R

Depth: Hole 875C, 0.14–105.5 mbsf; Hole 876A, 0.08–98 mbsf

Age: middle and late? Maastrichtian

Subunit IIA is a homogeneous, white (10YR 8/2), coarse skeletal grainstone (Fig. 6) that contains larger benthic foraminifers, rudist and red algal debris, and a few widely disseminated planktonic foraminifers. The grainstone is barely cemented; the preserved primary porosity has been enhanced by extensive dis-

solution. Grain size is coarse sand ( $1/2$  to 1 mm; 1–0  $\phi$ ) with minor variations to very coarse or medium sand. Sorting varies from poor to good, but it is generally moderate. Some grains are rounded, especially coarser ones. Many fragments, however, show the characteristic splitting along skeletal boundaries to produce more angular fragments with continued abrasion, known as the "Sorby effect" (Folk, 1967; Folk and Robles, 1964). This seems particularly true of radiolitic rudist fragments, which are typically angular. Admixtures of coarser skeletal debris produce intervals of floatstone (Interval 144-875C-4M-1, 33–44 cm) and rudstone (Intervals 144-875C-4M-1, 26–33 cm, and -4M-1, 50–72 cm; Intervals 144-876A-2R-1, 38–45 cm, -4R-1, 83–90 cm, -4R-1, 102–113 cm, and -7R-1, 0–4 cm), many represented by a single piece of core. The matrix of these coarser intervals remains coarse skeletal grainstone. Several intervals (Interval 144-875C-9M-1, 4–38 cm, and Intervals 144-876A-1R-1, 8–72 cm, and -3R-1, 0–19 cm) are packstone that contains only minor percentages of lime mud, distinctions that cannot be reliably made except in thin section. Further study will produce minor additions and deletions in this list. A significant occurrence of packstone forms the entire recovery below the manganese crust in Core 144-876A-1R (Interval 144-876A-1R, 8–76 cm). The matrix is formed by lithified pelagic ooze that contains Eocene planktonic microfossils ("Biostratigraphy" section, this chapter). Most of the planktonic foraminifers were filtered out by pore-throat constrictions within the top few centimeters. The mud fraction containing nannofossils reached at least 67 cm below the manganese crust, where it is reduced to 3 vol% perched on closely packed grains and within cavities. No pelagic matrix is present in the grainstones recovered from Site 875.

Larger benthic foraminifers, red algae, and rudist fragments are the major constituents of Subunit IIA (Table 3). Benthic foraminifers are robust and varied ("Biostratigraphy" section, this chapter); miliolids, characteristic mud lovers, are virtually absent. Red algae include lamellar encrusters, both corallineaceans and squamariaceans; many small fragments of encrusting and digitate forms; and widely scattered rhodoliths. Rudist fragments are mostly radiolitics, but they include some caprinids. Other recognizable bivalve fragments are sparse, and gastropods are conspicuously lacking (Table 3). Large fragments of coral and a few dasycladacean (green) algae are scattered throughout. Echinoderm fragments are a ubiquitous but small component, best seen in thin section; a few bryozoan fragments occur below 98.6 m in Subunit IIA. A minor, but highly significant, component of the skeletal grainstone from both sites is planktonic foraminifers (Fig. 7). These occur from Cores 144-875C-4M through -13M, and Cores 144-876A-7R through -14R ("Biostratigraphy" section, this chapter). The pelagic forms are of middle Maastrichtian age; they are contemporaneous with deposition, rather than infiltrated, because they occur only at depths >25 mbsf and are intimately intermixed with benthic forms in sheltered interstices and within muddy fills of skeletal cavities.

Extremely high porosity is characteristic throughout Subunit IIA (Fig. 8). Thin, discontinuous crusts of bladed calcite (PB<sub>3</sub>C; see "Explanatory Notes" chapter, this volume) have preserved the primary interparticle porosity (crBP; see "Explanatory Notes" chapter, this volume) and support most of the secondary molds (Fig. 8). The average cement content is  $5.3\% \pm 3.3\%$  in estimates from 30 thin-section samples (Table 4). These estimates include cement in both primary and secondary porosity. The moldic pores are rimmed by micrite envelopes (Fig. 8). The fragile mutual support of the envelopes and cement crusts has collapsed into rubble in some cases to produce either minor compaction or a unique kind of vug, where support by the surrounding grains is adequate for preventing collapse. Porosity estimates in slabbed cores are 10% to 30%, with a few intervals as low as 3%.

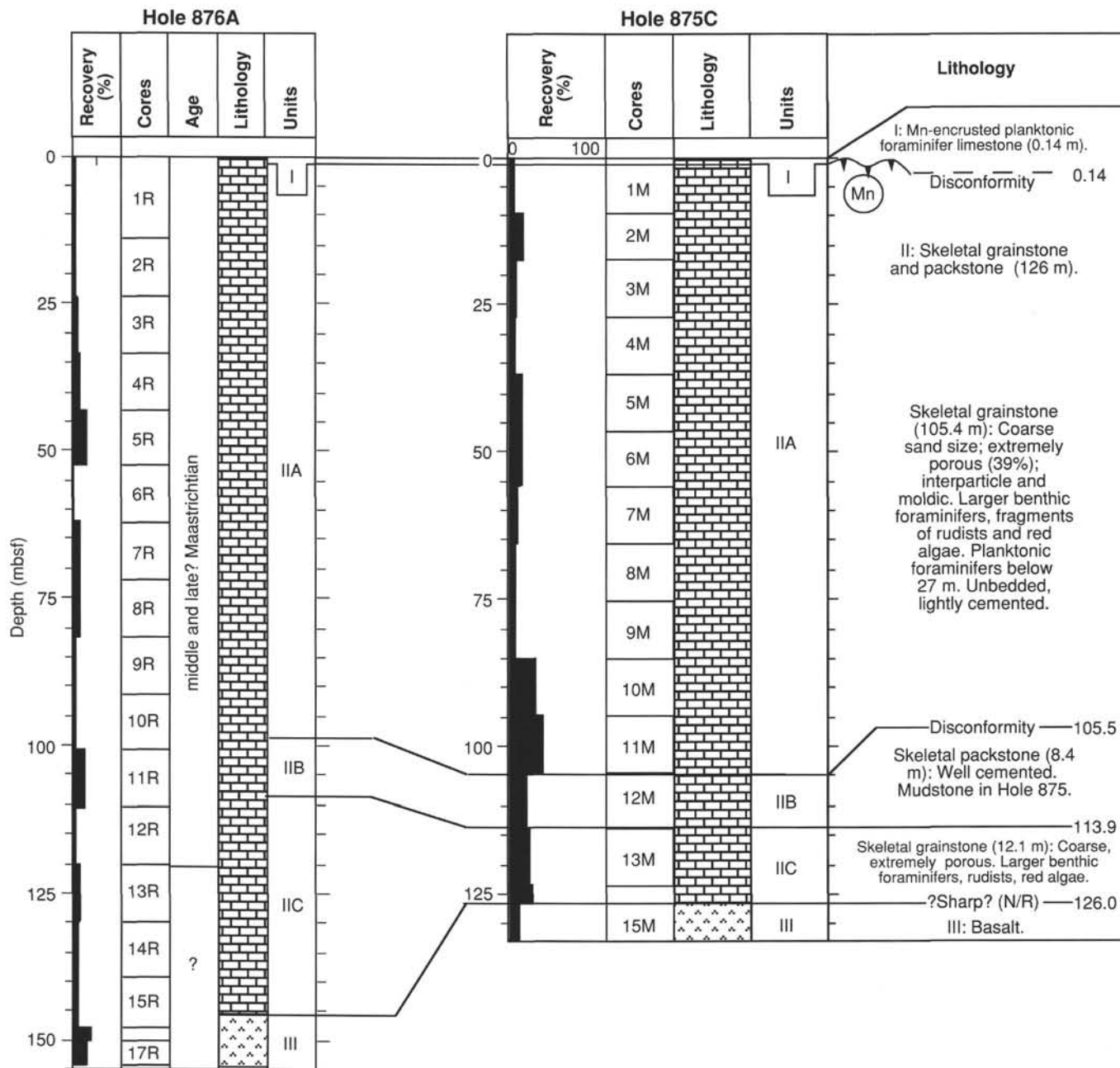


Figure 3. Lithostratigraphic correlation between Holes 876A and 875C. Depths are from Site 875.

Thin-section estimates and physical properties measurements have shown that these estimates are conservative. The average porosity from 22 measurements is  $39.4\% \pm 6.3\%$  (Table 2; see "Physical Properties" section, this chapter). About 56% of the porosity is primary interparticle and 44% is secondary, mostly as skeletal molds (Table 4). Some vugs are seen in cores and thin section, but these may have been produced by plucking of the saw or thin-section lapping. Larger vugs, if present, lead to drilling pebbles or rollers. Clear evidence of a cavity is present in Section 144-876A-1R-1, 43 cm, where probable contiguous surfaces of a cylinder and a roller are deeply etched and stained yellow (10YR 7/6). These core pieces were probably separated by a cavity of unknown dimensions, but larger than core diameter.

The upper contact of Unit II with the pelagic condensed interval of Unit I at about 0.1 mbsf is heavily encrusted by manganese.

Relief on the contact is demonstrated on small scale by about 6 cm of relief on the manganese crust in individual pieces (Fig. 4). Striking evidence of relief of at least 31 cm is provided by a vertical, manganese-stained contact between lithified skeletal sand of Unit II and pelagic limestone of Unit I (Interval 144-876A-1R-1, 25–39 cm; Fig. 9). No unequivocal borings or encrustations were noted on the contact. The vertical contact demonstrates that the skeletal sand was lithified, eroded, and filled by a matrix of pelagic ooze. This is a larger scale analog of the matrix infiltration described above that left Eocene nannofossils (see "Biostratigraphy" section, this chapter) resting on a thin crust of cement and occupying molds in Interval 144-876A-1R-1, 71–76 cm. These relationships signify that the skeletal sand was lightly lithified and solution etched to produce extensive moldic porosity before the Eocene.

**Subunit IIB**

Nature: cemented skeletal packstone

Intervals: Hole 875C, Sections 144-875C-12M-1, 125 cm, through -12M-2; Hole 876A, Sections 144-876A-10R-1, 0 cm, to -11R-2, 77 cm

Depth: Hole 875C, 105.5–113.9 mbsf; Hole 876A, 98–108 mbsf

Age: middle and/or late? Maastrichtian

Subunit IIB (Table 2) is a skeletal packstone with lenses of wackestone that is slightly muddier and much more cemented than the overlying and underlying grainstone subunits. A thin interval of distinctive gastropod lime mudstone was recovered from the middle of the subunit in Interval 144-875C-12M-2 at 15–33 cm.

The packstone and wackestone are white (10YR 8/2, in Hole 876A) or very pale brown (10YR 7/3, in Hole 875C). Mud content, estimated from seven thin-section samples, which includes only the packstone, ranges from 3% to 40%, with an average of 18%. Constituent grains are larger benthic foraminifers, fragments of red algae and rudists, a few coral fragments, and scattered planktonic foraminifers, which is essentially identical to the rest of the sand pile that comprises Unit II (Table 3). Distinctive constituents include large lamellar calcisponges (stromatoporoids), possibly encrusters, found at five or six intervals (Intervals 144-876A-11R-1, 60–64 cm, 120–125 cm, 129–131 cm, and 132–135 cm, and Interval 144-876A-11R-2, 42–46 cm). Scattered dark peloids are probably micritized red algal grains

**Table 2. Lithostratigraphic summary, Holes 875C and 876A.**

Unit/subunit	Cores	Depth (mbsf)	Age	Thickness (m)
Unit I	144-875C-1M-1, 0–14 cm	0–0.14	late middle Eocene	0.14
	144-876A-1R-1, 0–8 cm	0–0.08	through late Paleocene	0.08
Unit II	144-875C-1M-1, 14 cm, to -14M-1, 65 cm	0.14–126.0	middle and late	126
	144-876A-1R-1, 8 cm, to -15R-1, 12 cm	0.08–145.5	Maastrichtian to Campanian	145.5
Subunit IIA	144-875C-1M-1, 14 cm, to 12M-1, 125 cm	0.14–105.5	middle and late	105.4
	144-876A-1R-1, 8 cm, through -9R	0.08–98	Maastrichtian	98
Subunit IIB	144-875C-12M-1, 125 cm, through -12M-2	105.5–113.9	middle and late	8.4
	144-876A-10R-1, 0 cm, to 11R-2, 77 cm	98–108	Maastrichtian	10
Subunit IIC	144-875C-13M-1, 0 cm, to -14M-1, 65 cm	113.9–126.0	middle	12.1
	144-876A-11R-2, 77 cm, to -15R-1, 12 cm	108–145.5	Maastrichtian to Campanian	37.5
Unit III	144-875C-14M-1, 65 cm, to -15M-1, 77 cm	126.0–133.0	Unknown	??
	144-876A-15R-1, 12 cm, to 17R-1, 103 cm	145.5–154.0	Unknown	??

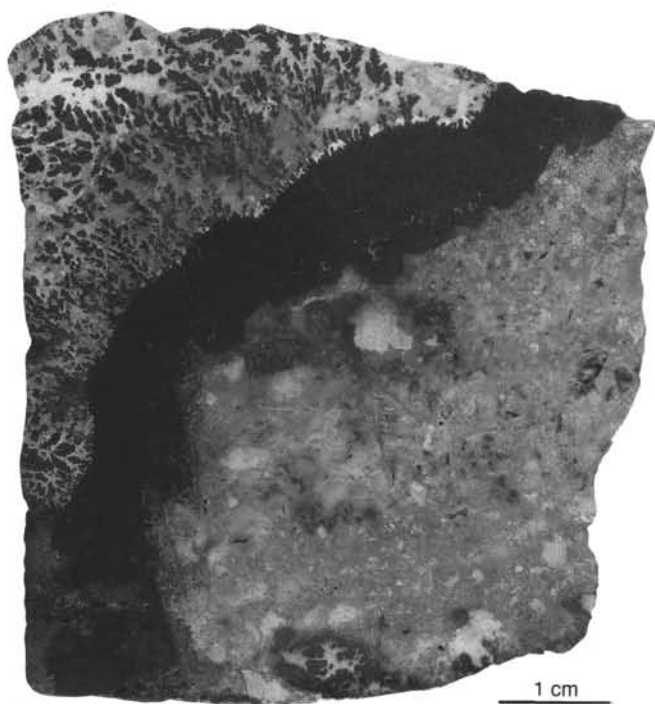


Figure 4. Close-up core photograph of manganese crust marking the contact between Unit I (top left) and Unit II (Interval 144-875C-1M-1, 0–6 cm). A similar contact was recovered in the underlying piece (see Fig. 5).

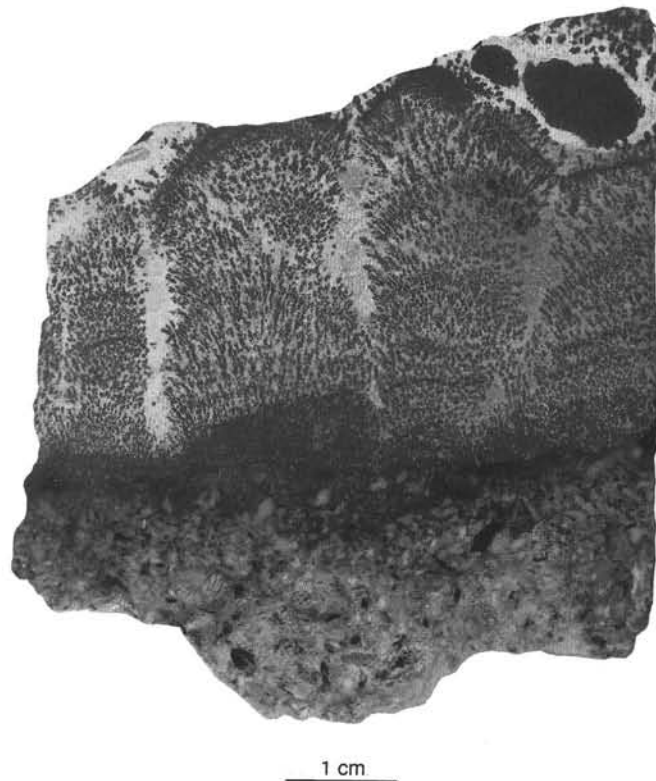


Figure 5. Close-up core photograph of columns of manganese dendrites extend into pelagic limestone from the contact between Unit I and the skeletal packstone of Unit II (Interval 144-875C-1M-1, 7–14 cm).

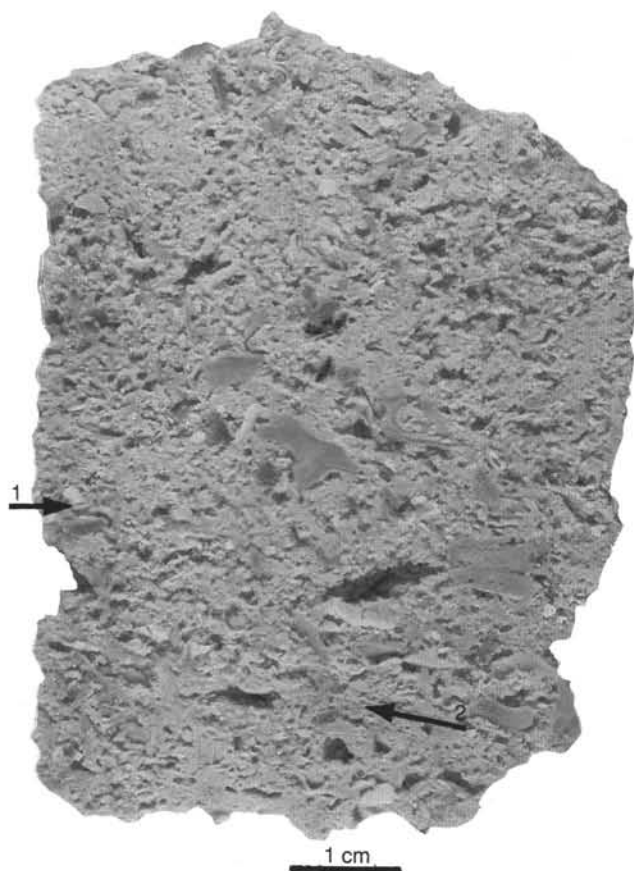


Figure 6. Close-up core photograph of porous skeletal grainstone (Interval 144-875C-2M-1, 15–23 cm). Coarser fragments are rudist bivalves, whereas white fragments are red algae (Arrow 1). Larger benthic foraminifer is shown by Arrow 2.

(Table 3). Presumed fecal pellets form thin packstone layers within a laminated cavity filling in Interval 144-876A-11R-2, 43–46 cm.

Porosity within the skeletal packstones is greatly reduced relative to the grainstones elsewhere in Unit II (Table 5). Three samples from Hole 876A average 5.8%; two samples from Hole 875C average 16%; the combined average for Subunit IIB is 9.9%

(“Physical Properties” section, this chapter; Table 5). Thin-section samples show that about 72% of the porosity is secondary (skeletal molds, Table 4). The low total porosity means that dissolution was retarded and grain interstices were filled relative to the adjacent grainstones. The matrix of lime mud partially or entirely occluded some interparticle pores and almost certainly reduced permeability (Enos and Sawatsky, 1981) and thus restrained dissolution. Cementation has also significantly reduced porosity and, probably, dissolution rates, as well as produced a much harder rock than that in the adjacent subunits. Cement averages  $21.1\% \pm 16.5\%$  in eight thin-section samples from the packstones of Subunit IIB.

Isopachous crusts of cloudy, bladed to fibrous cement are present in several thin sections from this interval. Several features within the cores indicate that cementation began during deposition. Isopachous cement is interlayered with and cements cavity-filling sediment (Interval 144-876A-11R-2, 43–46 cm; thin-section observation). Cementation beneath contacts, between slightly differing lithologies within the subunit, is indicated by a small, erect coral head that may encrust such a contact (Section 144-876A-10R-1, 30 cm) and by a scalloped surface having microrelief of 1 cm (Section 144-876A-11R-1, 40 cm). Well-cemented intraclasts of skeletal sand occur in the base of overlying Subunit IIA (Intervals 144-875C-12M-1, 112–118 cm, and -12M-1, 121–125 cm). Such critical features cannot generally be seen everywhere along a contact.

A thin layer of muddy, gastropod limestone (Interval 144-875C-12M-2, 15–33 cm) is unique to Subunit IIB. It includes a white (10YR 8/1), dense, unlaminated, 12-cm cylinder of lime mudstone (Fig. 10). Adjacent drilling pebbles of wackestone probably represent the same depositional episode. The mudstone contains small gastropod molds, ostracodes, and diminutive benthic foraminifers, mostly discorbids. No planktonic foraminifers were observed in this interval. Several burrows are filled with muddy packstone that contains larger benthic foraminifers, bivalve fragments, and coral fragments that are reminiscent of the adjacent packstones, as well as gastropods and mud (Fig. 10). Moldic porosity of 45% within the burrows (sxBU; see “Explanatory Notes” chapter, this volume) is also analogous to the adjacent packstones. The wackestone drilling pebbles contain gastropods (common), larger benthic foraminifers (many), corals (rare), dasycladacean algae (rare), and a gray-stained caprinid rudist fragment. Moldic porosity in the mudstone and wackestone is about 2%.

Unfortunately, no downhole logs were obtained at Sites 875 and 876, but drilling rates help constrain the intervals occupied by these denser, harder limestones (Table 5; see “Downhole

Table 3. Summary of thin section estimates of skeletal components as a percentage of bulk volume.

Hole and subunit		Foraminifers				Calcareous sponges	Corals	Gastropods	Bivalves	Radiolitics	Caprinids	Red algae	Green algae
		Planktonic	Larger	Other	Echinoderms								
Hole 875:													
Subunit IIA	Average	0.18	14.67	0	3.89	1.28	2.78	0.11	13.17	5.50	1.33	9.50	0.30
Subunit IIB	Average	0.70	15.00	2.67	1.00	0.03	0	0	8.00	4.67	0	6.67	0
Subunit IIC	Average	0.39	13.75	0	4.63	0.13	0.75	0.14	10.25	4.13	0	15.00	0
Hole 876:													
Subunit IIA	Average	0	8.75	1.42	3.00	0	4.17	0	10.67	5.17	0.08	14.42	0
Subunit IIB	Average	0	13.83	0.85	2.17	5.00	1.50	0.17	2.50	0.17	1.00	4.67	0
Subunit IIC	Average	0	16.00	0.03	3.75	1.00	0	0.75	14.00	0	0	10.50	0
Holes 875 and 876:													
Subunit IIA	Average	0.26	12.06	0.55	3.45	0.74	3.23	0.06	11.77	5.19	0.81	11.42	0.17
	SD	0.93	7.12	2.71	2.53	3.95	8.92	0.25	7.43	6.18	1.74	7.30	0.91
Subunit IIB	Average	0.23	14.22	1.46	1.78	3.34	1.00	0.11	4.33	1.67	0.67	5.33	0
	SD	0.66	11.95	2.78	1.86	8.29	2.65	0.33	5.10	3.94	2.00	3.97	0
Subunit IIC	Average	0.26	14.50	0.01	4.33	0.42	0.50	0.34	11.50	2.75	0	13.50	0
	SD	0.86	8.22	0.03	3.50	1.16	1.45	0.88	9.90	4.94	0	5.98	0

Notes: For number of samples in each subunit, see Table 4. Bivalve abundance includes rudists (radiolitics and caprinids). SD = standard deviation.

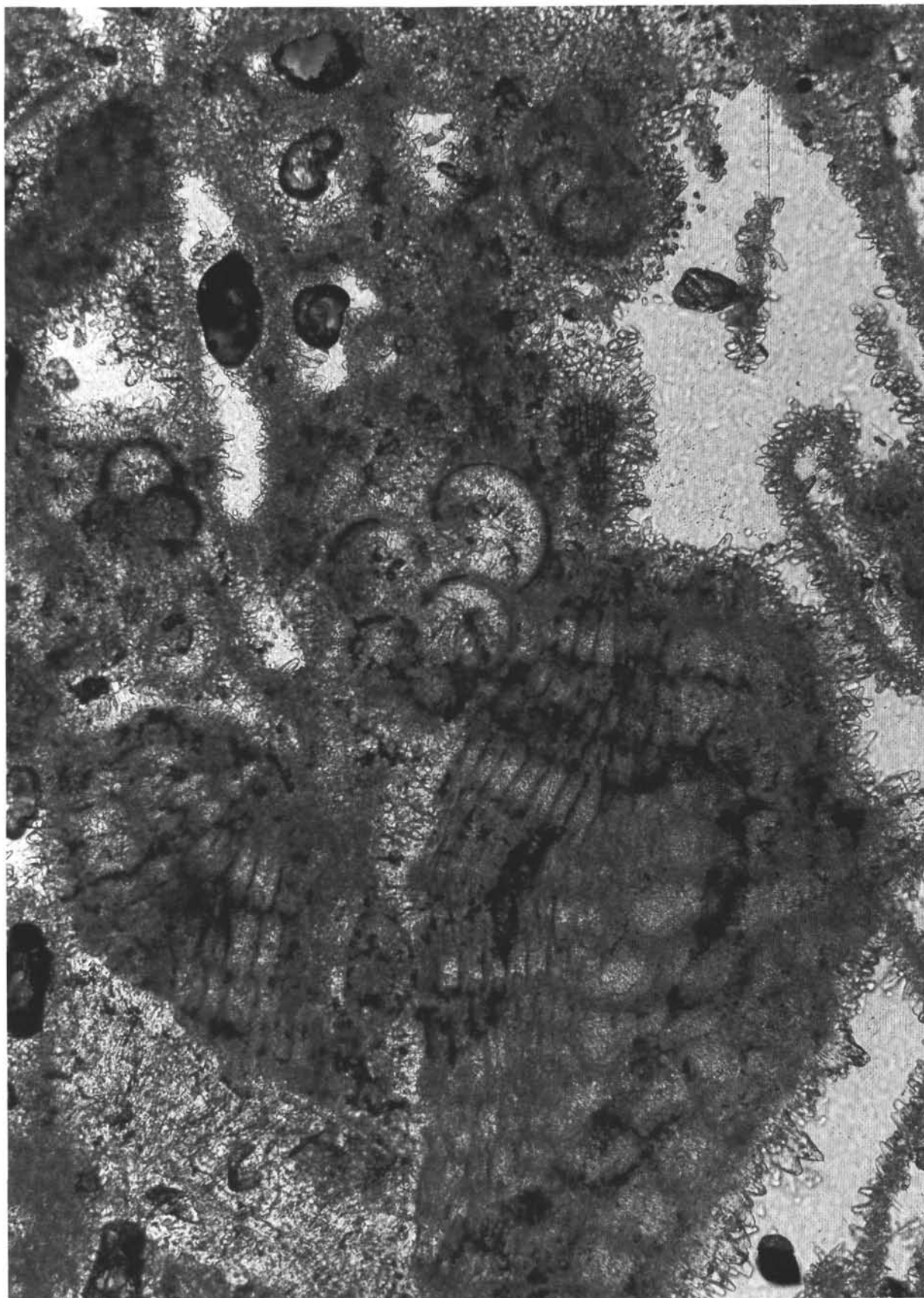


Figure 7. Thin-section photomicrograph (plane light) of pelagic foraminifers nestling with larger benthic foraminifers in the skeletal packstone of Subunit IIA (Interval 144-875C-5M-1, 131-136 cm). Maximum dimension is 1.5 mm.

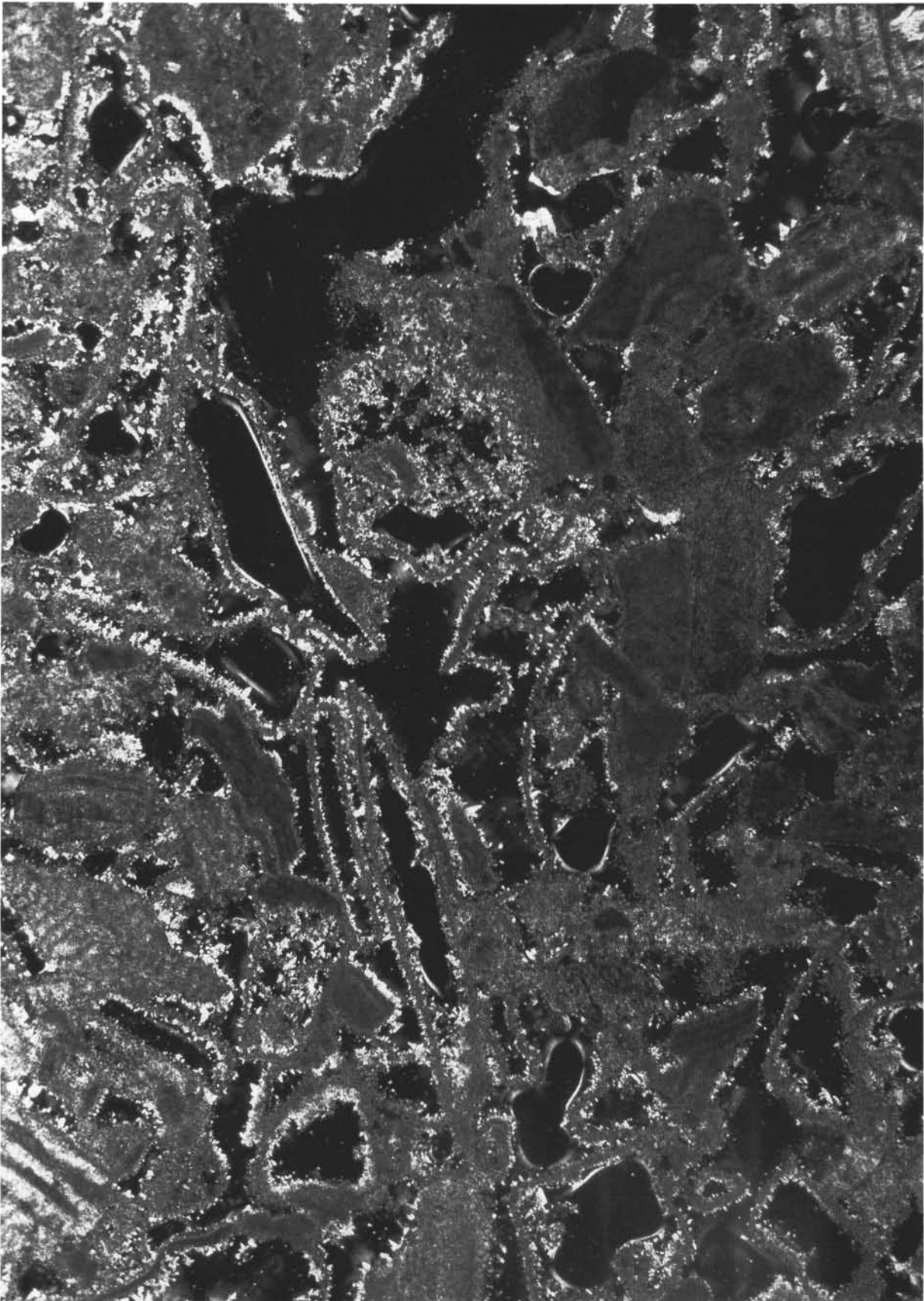


Figure 8. Thin-section photomicrograph (crossed polars) of extreme moldic porosity supported by micrite envelopes and minimal calcite cement in Subunit IIA (Interval 144-875C-1M-1, 34–36 cm). Maximum dimension is 6 mm.

**Table 4. Summary of thin section estimates of nonskeletal components as a percentage of bulk volume.**

Hole and subunit	Number	Mud	Peloids	Cement	Porosity (%)	Secondary (%)
<b>Hole 875:</b>						
Subunit IIA Average	18	6.28	2.28	5.50	38.50	44
Subunit IIB Average	3	44.00	1.00	3.00	16.67	70
Subunit IIC Average	8	15.25	0.75	16.38	18.50	74
<b>Hole 876:</b>						
Subunit IIA Average	12	7.21	3.43	5.33	35.25	27
Subunit IIB Average	6	16.67	15.00	26.67	5.00	73
Subunit IIC Average	4	5.00	0.50	16.00	22.00	50
<b>Holes 875 and 876:</b>						
Subunit IIA Average	30	6.85	2.62	5.26	37.20	43
SD		6.85	3.52	3.27	9.07	11
Subunit IIB Average	9	25.78	10.33	21.13	8.50	72
SD		28.59	12.38	16.94	12.96	27
Subunit IIC Average	12	11.83	0.67	16.25	19.67	70
SD		15.04	1.50	13.69	13.36	28

Notes: Mud includes mud matrix and some micrite envelopes. Peloids include some fecal pellets, but most are probably skeletal grains altered beyond recognition. Secondary porosity (molds and vugs) is percentage of total porosity. SD = standard deviation.

Measurements and Seismic Stratigraphy" section, this chapter). A slight reduction in drilling rate at about 97.5 mbsf in Hole 876A coincides approximately with the top of the cemented packstone and wackestone at Section 144-876A-10R-1, 0 cm. The drilling rate increased for the next several meters, followed by a spike of slow drilling at 106 mbsf and several more meters of slightly reduced rates (see "Downhole Measurements and Seismic Stratigraphy" section, this chapter). In Hole 875C, an interval of about 6 m of slow drilling within Core 144-875C-12M includes a spike at 110.5 mbsf that speculatively coincides with the mudstone layer.

The contact with the overlying porous grainstones of Subunit IIA has been placed at the uppermost well-cemented packstone interval in Hole 875C (Section 144-875C-12M-1, 125 cm), which is overlain by intraclast rudstone (Intervals 144-875C-12M-1, 121–125 cm, and -12M-1, 112–118 cm). The contact within Hole 876A may fall between Cores 144-876A-9R and -10R, although an apparently minor contact at Section 144-876A-10R-1, 4 cm (or another within the core) might be more significant than is apparent in the visual core description.

### Subunit IIC

Nature: porous skeletal grainstone

Intervals: Hole 875C, Section 144-875C-13M-1, 0 cm, to -14M-1, 65 cm; Hole 876A, Sections 144-876A-11R-2, 77 cm, to -15R-1, 12 cm

Depth: Hole 875C, 113.9–126.0 mbsf; Hole 876A, 108–145.5 mbsf

Age: possibly Campanian to middle or late? Maastrichtian

Skeletal grainstones having minimal cement and high porosity underlie Subunit IIB and extend to the basalt at the bottom of both Holes 875C and 876A (Table 2). In most respects, this lithology is identical to that of Subunit IIA. It is mostly white (10YR 8/2), but there are several intervals of varying shades of very pale brown (10YR 7/3, 8/3, and 8/4). Grain size is coarse sand. Some intervals have small admixtures of mud (packstones) or coarser grains. Likewise, the main constituents are larger benthic foraminifers, red algae, and rudist fragments (Table 3). Planktonic foraminifers are scattered throughout.

Porosity is high (30.9%) in Subunit IIC, somewhat less than that in Subunit IIA (39.4%; Table 5). Secondary porosity (molds and some vugs) is more abundant than primary interparticle porosity (Table 3). Calcite cement is considerably more extensive, with an average of  $16.3\% \pm 13.7\%$  in 12 thin-section samples from

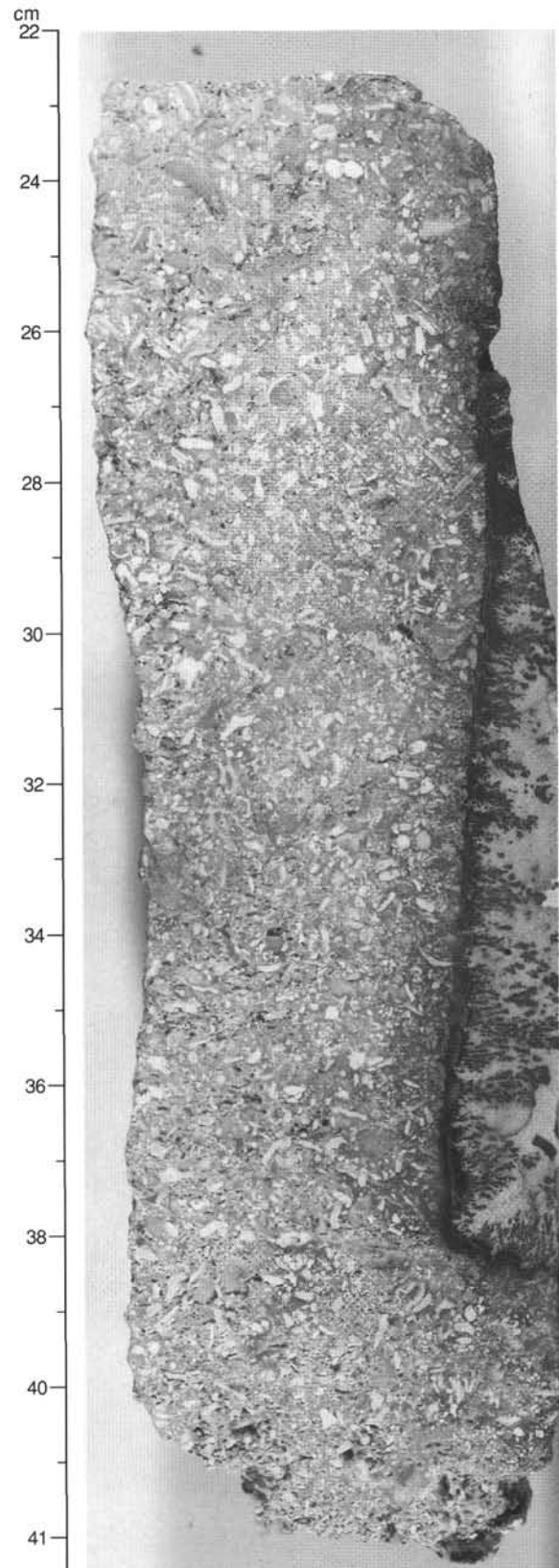


Figure 9. Close-up core photograph of vertical manganese-encrusted contact between lithified pelagic ooze of Unit I (right) and lithified skeletal sand of Unit II (left) (Interval 144-876A-1R-1, 22–41 cm).

**Table 5. Porosity and drilling rates of skeletal grainstones and packstones from Sites 875 and 876.**

Subunit	Lithology	Hole 875C	Hole 876A	Total
Subunit IIA	Grainstone			
Average porosity (%)		38.8	40.1	39.4
Standard deviation		±4.1	±8.9	±6.3
Range		31.6–46.4	24.0–47.2	24.0–47.2
Subunit IIB	Packstone and mudstone			
Average porosity (%)		16.1	5.8	9.9
Standard deviation		—	±1.3	±5.8
Range		15.4–16.8	4.4–6.9	4.4–16.8
Drilling rate (int. ave.)		5.8	5.8	5.8
Standard deviation		±5.5	±7.3	±6.4
Range (min/m)		1.5–18.0	1.0–24.0	1.0–24.0
Subunit IIC	Grainstone			
Average porosity (%)		28.8	35.1	30.9
Standard deviation		±8.0	—	±7.5
Range		19.1–37.4	30.6–39.5	19.1–39.5

Note: (int. ave.) = (internal average).

Subunit IIC. Some more-cemented intervals were noted in visual core descriptions (e.g., Interval 144-876A-13R-1, 40–119 cm). Cements seen in thin section include clear calcite overgrowths on echinoderms, some foraminifers, and unidentified grains and equant crystals that fringe primary and secondary pores. Either cement type may occupy as much as 20% of different thin-section samples.

A thin interval of muddy clasts breaks the monotony of the skeletal grainstones (Interval 144-875C-13M-1, 66–72 cm; Fig. 11). These clasts are laminated, fine-grained wackestones and possibly mudstones. They are set in a somewhat grainier matrix (packstone and wackestone) that has developed a lamination draping around the clasts. Bending of the clasts and blurred margins suggest that they were unlithified when deposited. Clast margins could not be distinguished in a small thin section, but a hint of binding was evident in layers of horizontally oriented bioclasts interwound with red algae and calcisponges. The clasts overlie porous packstone on an erosion surface marked by truncated grains and red algal encrustation (Fig. 11).

Another slight variant is that of intervals with distinctly browner, albeit still very pale (10YR 8/3 and 7/3), to brownish yellow (10YR 6/6), slightly finer (medium and coarse sand), and lightly cemented grainstone. Two such intervals occur in Hole 876A (Intervals 144-876A-13R-1, 0–33 cm, and -14R-1, 0–83 cm) and one in Hole 875C, immediately overlying basalt (Interval 144-875C-14M-1, 18–62 cm).

In Hole 875C, a few small basalt fragments are incorporated in Interval 144-875C-14M-1, 62–65 cm. Below this interval, the hole passes into the basaltic lava of Lithologic Unit III at 124.3 mbsf. In Hole 876A, several altered basalt pebbles were recovered at the limestone-basalt interface near 139.5 mbsf (Interval 144-876A-15R-1, 12–18 cm). Some of these are enclosed by a lithified limestone matrix. The pebbles are subangular to subrounded in shape and 1–2 cm in size.

The thickness of Subunit IIC increases threefold, from 12.1 m in Hole 876C to 37.5 m in Hole 875C. The base of the subunit may be as old as Campanian or as young as Maastrichtian at the bottom of each hole (see “Biostratigraphy” section, this chapter).

The contacts between Subunits IIB and IIC occur in intervals that were not recovered (Hole 875C) or within drilling pebbles (Hole 876A). The contact of Unit II limestone with basalt was seen within a core at each site (Cores 144-875C-14M and 144-876A-15R); it appears to be sharp. Notably absent are the clays that intervened at Sites 873, 874, and 877 on Wodejebato Guyot.

## Unit III

Nature: basalt

Intervals: Hole 875C, Sections 144-875C-14M-1, 65 cm, to -15M-1, 77 cm; Hole 876A, Sections 144-876A-15R-1, 12 cm to -17R-1, 103 cm

Depth: Hole 875C, 126.0–133.0 mbsf; Hole 876A, 145.5–154.0 mbsf

Age: unknown

Drilling in Holes 875C and 876A ended after less than 10 m of basalt was cored (see “Igneous Petrology” section, this chapter).

### Preliminary Interpretation of Depositional History

Several observations concerning the setting and lithology of Sites 875 and 876 place constraints on their interpretation. Both sites are located on the same prominent bathymetric ridge, about 1.7 km wide, concentric with the outline of Wodejebato Guyot, and about 45 m lower in elevation than the morphologically analogous inner ridge where Sites 874 and 877 were located (Fig. 4; see “Underway and Site Geophysics” section, “Site 874” chapter, this volume). At this location, a buttress-like shelf (“rift zone”) projects northeastward from the guyot. Correlations between Sites 875 and 876, located only 1.6 km apart, are straightforward, confirming the initial premise that they are on depositional strike. The outer ridge is a persistent, but apparently discontinuous, feature around the north and east sides of the guyot (Bergersen, in press; see “Underway and Site Geophysics” section, “Site 874” chapter, this volume). This implies that the rocks encountered at Sites 875 and 876 are not just a local feature; analogous rocks are to be expected at analogous locations elsewhere on the guyot. On the other hand, the discontinuity of the outer ridge, unless caused by faulting, implies that the facies belt is discontinuous. The absence of either of the prominent ridges on the southern margin of the guyot has been attributed to faulting (see “Underway and Site Geophysics” section, “Site 874” chapter, this volume); thus, the overall continuity or any asymmetry in the facies cannot be evaluated.

The morphologic similarity of the two ridges led to the expectation before drilling at Site 875 that the outer ridge would be a “reef” or shelf-margin facies comparable with those encountered at Site 874 and eventually at Site 877. This led to the further premise that the two ridges, roughly concentric, 1 km apart, and differing by 45 m in elevation, would also differ in age. Thus, it was a considerable surprise to encounter only skeletal sands at Sites 875 and 876. Moreover, they are coeval with the rocks recovered from Sites 874 and 877, within the limits of biostratigraphic resolution.

The sand pile encountered at Sites 875 and 876 contains abundant fragments of typical Late Cretaceous reef organisms, notably rudist bivalves, red algae, and a few corals; however, the dominant constituent overall is that of larger benthic foraminifers. Planktonic foraminifers occur in most cores, except near the top of the sequence. Conspicuously absent are gastropods and miliolid foraminifers, the forms most typical of lagoons or other slightly restricted settings.

The sands of Subunits IIA and IIC are well-washed, moderately sorted, and somewhat rounded. Although debris of reef organisms is abundant, no blocks of any type of boundstone or other reef lithology were encountered. The few clasts recovered are intraclasts of cemented sand or unlithified mud. No trace of

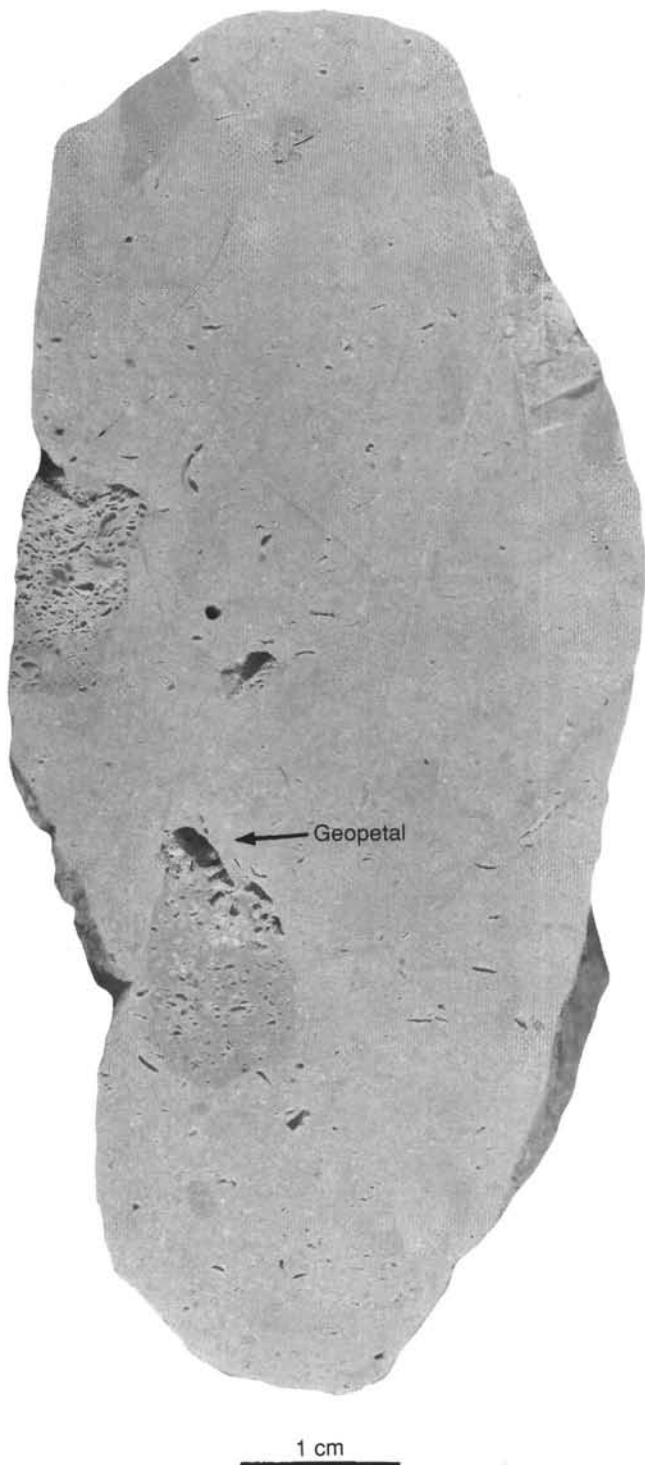


Figure 10. Close-up core photograph of burrowed gastropod mudstone of Unit IIB (Interval 144-875C-12M-2, 21–30 cm). Burrows are filled with muddy packstone. Note the geopetals at the tops of burrows.

bedding or hydrodynamic structures were visible in the cores, although bedding is not always apparent in unweathered, well-sorted sands. A six-channel seismic profile through Site 875 indicates a slight seaward dip of reflectors (Fig. 3, see “Underway and Site Geophysics” section, “Site 874” chapter, this volume).

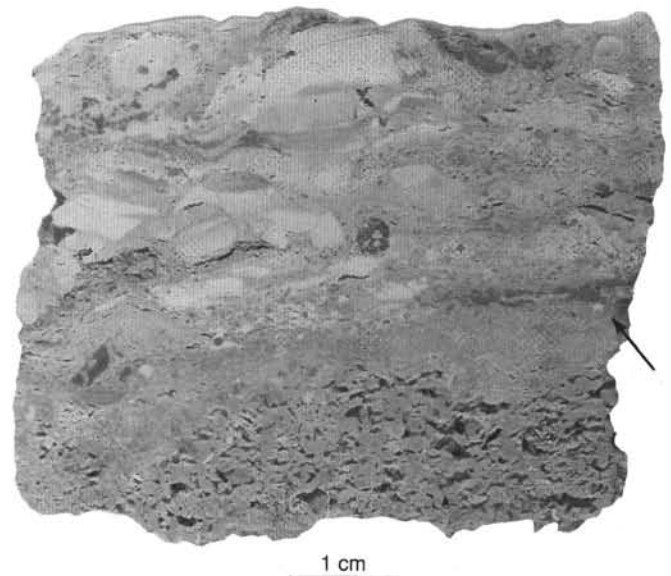


Figure 11. Close-up core photographs of muddy clasts overlying lithified grainstone (Interval 144-875C-13M-1, 67–72 cm). The contact (arrow) is marked by truncated grains and red algal encrustation.

The texture and composition of the sands are what might be expected leeward of a reef or any productive shelf margin, far enough leeward for both coarse and fine fractions to be removed. The line of sandy cays that marks modern atolls would be such a setting. The dominance of larger foraminifers is consistent with this setting (McKee et al., 1959). This possibility seems precluded by the location of the sands seaward of the apparently contemporaneous reef and at the very margin of the guyot. Unless faulting or erosion has altered the record, probably no source of shallow-water skeletal debris existed seaward of the sand pile at Sites 875 and 876.

The obvious choice of settings for deposition of the skeletal sands is as a fore-reef apron, seaward of the reef tract of the inner ridge probed at Sites 874 and 877. This tract forms an obvious upslope source for the sands, although the initial depositional surface, indicated by depth to basement, was nearly flat. Indeed, the sands in the lower part of the sequences at Sites 874 and 877 are similar to those at Sites 875 and 876, except perhaps slightly less washed and sorted. The most obvious difference is the persistent occurrence of planktonic foraminifers at Sites 875 and 876. This occurrence is consistent with deposition on a fore-reef apron at modest depths.

This choice of environments raises a number of questions. One is the absence of any coarser reef debris. Some indications of both organic binding and penecontemporaneous cementation at Sites 874 and 877 are evident. In an open-ocean setting adjacent to a steep slope, the expectation is that considerable coarse rubble would be transported onto a fore-reef apron, if the inner and outer ridge sequences are indeed synchronous.

The degree of washing, rounding, and sorting of the sediment, even the abrasion-induced angularity of some skeletal debris, suggests that the sands underwent considerable reworking, presumably by waves or currents in shallow water, before reaching the depositional milieu. Transport directly from a reef does not provide for this reworking.

The surface morphology also raises questions. A trough about 50 m deep now separates the two ridges. This trough appears to open to the southeast where the outer ridge becomes deeper and less prominent. The two ridges come closer together and are less

pronounced toward the northwest. If the trough is of depositional origin, it would have precluded transport of sediment directly seaward from the reef. If it is a more recent feature, how did it originate? Why do two concentric ridges appear intermittently around the east and north margins of Wodejebato Guyot? Any explanation of origin must be a general one.

Although these questions cannot be satisfactorily answered with the present information, the sands recovered at Sites 875 and 876 most likely accumulated in a fore-reef position at some depth below the reef and below sea level. A few planktonic organisms drifted onto the sand pile, which was probably reworked by burrowers. This mixed in the plankton and destroyed any sedimentary structures that might have provided further clues to the depositional setting.

Subunit IIB, skeletal sands with some mud and considerable cement, punctuated the deposition of well-winnowed skeletal sand that remained unlithified in Subunits IIA and IIC. The isopachous crusts of cloudy, fibrous-to-bladed cement found in several samples from Subunit IIB have been interpreted as submarine cement on the basis of cement morphology, interlayering with marine sediment, and the sedimentologic evidence for pencontemporaneous cementation outlined above. This was the first step in the advanced lithification of Subunit IIB, although it is not the entire story. Other, later cements are present, and not all samples examined show evidence of early marine cementation.

The presence of both marine cement and mud suggests a reduced rate of sedimentation and/or a reduction in energy ("Grains that lay together stay together."—R.N. Ginsburg, pers. comm., 1965). Several causes are possible for such changes; for example, decreased productivity in the shallow-water sediment source or changes in depth.

The origin of the mudstone interval within the skeletal sands of Subunit IIB at Site 875 poses other constraints. The fauna of gastropods, ostracodes, and diminutive foraminifers as well as the muddy texture reflect restricted conditions, probably in shallow water. This conclusion is supported by the absence of planktonic foraminifers in this interval. Thus, a period of shoaling, perhaps abrupt, with establishment of restricted conditions is indicated. The alternative explanation, that the structureless mud and sparse biota were transported to this setting, say from the lagoon, appears unlikely, although the incomplete recovery obscures the issue. No admixture of skeletal sand can be found in the mudstone, except in burrows. No other similar rocks were recovered, as might be expected if a conduit for sediment from the lagoon was present. Finally, this lithology is not typical of the lagoonal deposits from Wodejebato Guyot (see "Lithostratigraphy" section, "Site 873" chapter, this volume).

The potential correlation of this interval to other sites on the guyot is a key question. Facets of the diagenetic history discernible from preliminary study are relevant to the depositional history. The occurrence of probable submarine cement within Subunit IIB is part of the extensive lithification characteristic of this subunit. The contact between Subunits IIA and IIB may be a submarine hardground, for example, at the contact observed at Section 144-876A-10R-1, 4 cm.

The contact between Unit I, the manganese-impregnated late Paleocene pelagic limestone, and the Maastrichtian skeletal grainstone of Unit II is marked by at least 31 cm of relief (Fig. 9) and by infiltration of pelagic ooze into lightly cemented, moldic, skeletal sand for at least 70 cm below the contact. A relief of about 1 m on unconnected depressions in the manganese-encrusted surface of the limestone was seen in the VIT survey at peripheral ridge sites. This surface, perhaps a microkarst, probably formed between late Maastrichtian and late Paleocene time. The surface relief might also reflect depositional topography or subsequent bioerosion, although no boring or encrustation of the contact is

evident. In any event, the skeletal sands were lightly lithified and skeletal molds were developed before submergence into the pelagic realm by the late Paleocene. That is essentially its diagenetic stage to the present day, although it is by no means certain that all of the cements and molds formed before late Paleocene time.

## BIOSTRATIGRAPHY

### Introduction

Sites 875 and 876 were drilled on the outer ridge of the summit of Wodejebato Guyot along its northwestern perimeter; Site 876 lies 1.67 km northwest of Site 875. A 126- to 145-m-thick sequence of skeletal grainstones (Lithologic Unit II), mainly of middle and late? Maastrichtian age, rests directly on basalt at these sites. The grainstone sequence comprises carbonate sands and contains benthic foraminifers throughout as well as planktonic foraminifers in most samples. The grainstones are overlain by a thin manganese-encrusted and phosphatized pelagic limestone (Lithologic Unit I) investigated biostratigraphically at the millimeter scale using nannofossils and planktonic foraminifers. These fossils reveal a long and complex history of early Tertiary pelagic sedimentation and erosion that took place after the guyot had submerged below deep waters.

Three holes were drilled at Site 875. Holes 875A and 875B were aborted after reaching total depths of 11.2 and 40.0 m, respectively. Hole 875C ended in basalt at 133.0 mbsf, with core recovery averaging 13.2%. A single hole (Hole 876A) was drilled to a total depth of 154.0 mbsf at Site 876, which also ended in basalt. Core recovery for this hole averaged 9.6%. The biostratigraphic results for Holes 875C (see Figs. 12–13) and 876A (see Fig. 14) rely exclusively upon calcareous microfossil occurrences.

The lithologies recovered in Holes 875C and 876A are comparable and allow the same lithostratigraphic units and subunits to be recognized at both sites.

### Calcareous Nannofossils

#### *Manganese-encrusted and Phosphatized Pelagic Limestone (Lithologic Unit I)*

##### *Hole 875C*

Sample 144-875C-1M-1, 4–6 cm, consists of manganese crust/dendrites and phosphatized pelagic limestone. The pelagic limestone from this sample contains an abundant, uniform assemblage including *Discoaster barbadiensis*, *D. saipanensis*, *Sphenolithus intercalaris*, *Reticulofenestra dictyoda*, *R. umbilica*, and *Chiasmolithus grandis*. The presence of *R. umbilica*, *C. grandis*, and *S. intercalaris* without *Discoaster bifax* and *Chiasmolithus solitus* indicates Subzone CP14b of late middle Eocene age. Preservation is good to moderate, with some overgrowth on the discoasters. Two specimens of reworked Cretaceous nannofossils—*Watznaueria barnesae* and *Lithastrinus grillii*—were observed in this sample. The biostratigraphic distribution of these two species limits their provenance to pelagic sediments of Santonian or Campanian age.

Sample 144-875C-1M-1, 0–2 cm, consists of a complex sequence of breccias, manganese crusts, and pelagic limestone fillings. Phosphatization and the invasion of manganese dendrites has severely altered parts of this sediment, whereas others are little affected by diagenetic processes. Although the thin section is too thick in most parts to examine nannofossils, at least two different zones were observed.

The younger zone is the combined CP11–CP12a zone (late early Eocene). It is characterized by the presence of *Discoaster lodoensis*, *D. kuepperi*, and *Reticulofenestra dictyoda* without *Rhabdosphaera inflata* or *Reticulofenestra umbilica*. The pres-

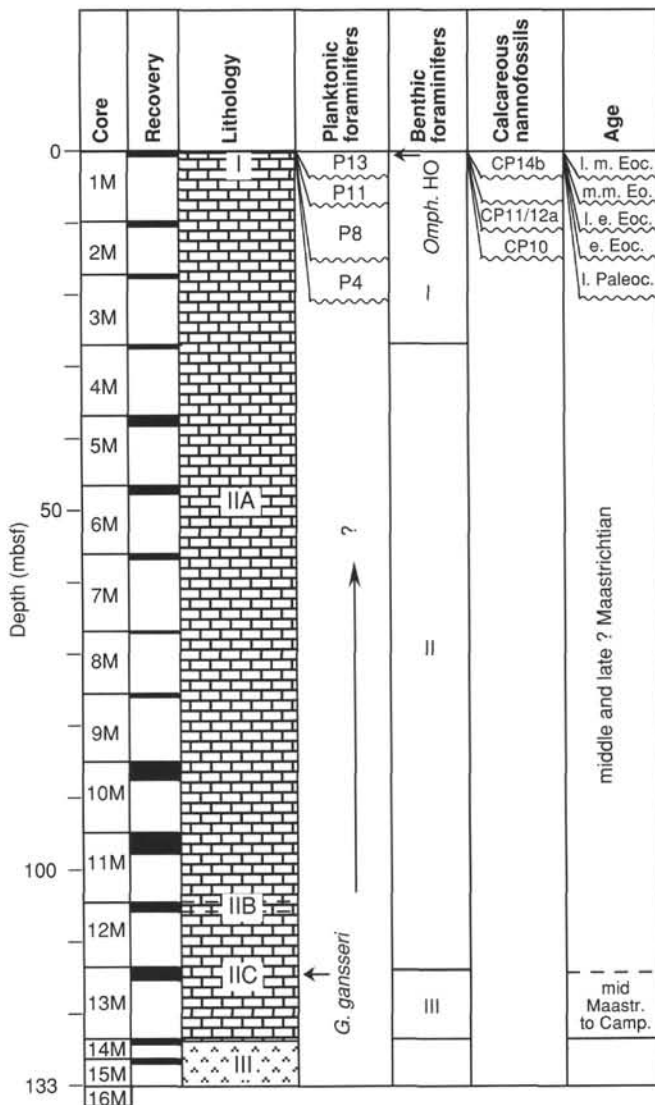


Figure 12. Biostratigraphy of Hole 875C, Wodejebato Guyot. Core recovery is shown as black bars. Lithologic units and subunits are superimposed on the "Lithology" column. In the "Benthic foraminifers" column, the highest occurrence of *Omphocyclus* is abbreviated to "Omph." HO.

ence or absence of *Discoaster sublodoensis* could not be reliably established in this thin section, hence the combined zonal attribution. The CP11–CP12a combined zone occurs as irregular patches throughout the thin section; some of these may be burrows, others are clearly cavity fills.

The older zone identified by nanofossils in Sample 144-875C-1M-1, 0–2 cm, is Zone CP10 (early Eocene), indicated by the presence of *Discoaster lodoensis*, *Discoaster kuepperi*, and *Tribrachiatus orthostylus*. Two distinct, repetitive assemblages were observed within this biostratigraphic interval. The first, and presumably older, assemblage is characterized by *Neococcolithes protenus*, *Toweius gammaton*, and *Scyphosphaera tubicena*, in addition to *D. lodoensis* and *D. kuepperi*. Its older age is based on the stratigraphic range of *N. protenus*, which becomes extinct in the lower part of Zone CP10 (Perch-Nielsen, 1985). This well-preserved assemblage occurs as irregular void fills within the manganese crust. The second, presumably younger, assemblage is characterized by *Lophodolichus mochloporus*, *L. nascens*, and *Pseudotriquetrorhabdulus inversus*, in addition to *D. lodoensis*,

*D. kuepperi*, and *T. orthostylus*. This assemblage occurs as distinct, polygonal, manganese-rimmed clasts surrounded by a matrix of CP11–12a pelagic limestone, indicating a disconformable relationship between the CP10 clasts and the CP11–12a matrix.

#### Hole 876C

Three thin-section samples of manganese crusts from Interval 144-876A-1R-1, 8–37 cm, were examined for nanofossils, as follows.

Sample 144-876A-1R-1, 8–17 cm, contains nanofossil assemblages from two zones. The older material contains *Discoaster lodoensis*, *D. kuepperi*, *Reticulofenestra dictyoda*, and *Sphenolithus editus*, indicating Zone CP10 of early Eocene age. This assemblage is very well preserved and is characterized by the presence of many intact coccospheres, largely of *Coccolithus pelagicus* s.l. In addition, this assemblage contains abundant *Thoracosphaera saxea* s.l., which are sometimes tightly packed, forming a thoracospherid grainstone/packstone. Zone CP10 material occurs within the manganese crust and between manganese dendrites, implying that it is at least partially coeval with the deposition of the manganese. This sample also includes a late middle Eocene age assemblage (Subzone CP14a) characterized by *Reticulofenestra umbilica*, *Chiasmolithus grandis*, *C. solitus*, and *Sphenolithus furcatolithoides*. This assemblage is beautifully preserved, with many of the *R. umbilica* retaining their fragile central nets in exceptional detail. This material forms a fill surrounding the manganese crust.

Sample 144-876A-1R-1, 17–21 cm, contains void fillings of pelagic limestone with nanofossils, including *Discoaster lodoensis*, *D. kuepperi*, *Chiasmolithus solitus*, *Sphenolithus editus*, and *Neococcolithes protenus*. This assemblage indicates Zone CP10 of early Eocene age. All void fillings that could be observed appear to contain assemblages of uniform composition, although many parts of the thin-section sample were either too thick or too heavily phosphatized to discern any characteristic nanofossils.

Interval 144-876A-1R-1, 23–42 cm, consists of a nearly vertical sided cavity in the skeletal grainstone that was coated by manganese crust and filled with pelagic limestone (Fig. 14). The thin section of Sample 144-876A-1R-1, 36–37 cm, reveals a complex history of deposition within this cavity. The sample is divided roughly in half by a prominent manganese crust. Dendrites from this crust extend inward (into the former cavity) nearly to the edge of the thin-section sample. Beneath the crust and proximal to the outer wall of the former cavity, Cretaceous platform debris and phosphatized clasts of uncertain age are contained within a matrix of pelagic limestone bearing very well-preserved nanofossils. The presence of *Discoaster lodoensis*, *D. binodosus*, *D. kuepperi*, *Sphenolithus editus*, and *Ellipsolithus distichus* indicate Zones CP10 of early Eocene age. Within the manganese crust, and between the dendrites for most of their extent, is a significantly younger assemblage characterized by *Reticulofenestra dictyoda*, *Sphenolithus spiniger*, *S. furcatolithoides*, and *Chiasmolithus grandis* without *Reticulofenestra umbilica*. This association of species indicates Zone CP13 of middle Eocene age. This assemblage is generally moderately to poorly preserved, with most of the placoliths exhibiting significant etching. The edge of the thin-section sample (distal to the wall of the former cavity) consists of an irregular patch (varying from 0 to 1 mm wide) of pelagic limestone containing *Reticulofenestra umbilica*, *Discoaster saipanensis*, *Sphenolithus spiniger*, and *Chiasmolithus grandis*, indicating Subzone CP14a of late middle Eocene age. The CP14a assemblage is moderately to well preserved.

A cavity infilling in Sample 144-876A-1R-1, 71–76 cm, contains a moderately preserved, sparse nanofossil assemblage including *Discoaster barbadiensis*, *D. strictus*, and *D. bifax*, indicating Subzone CP14a of late middle Eocene age.

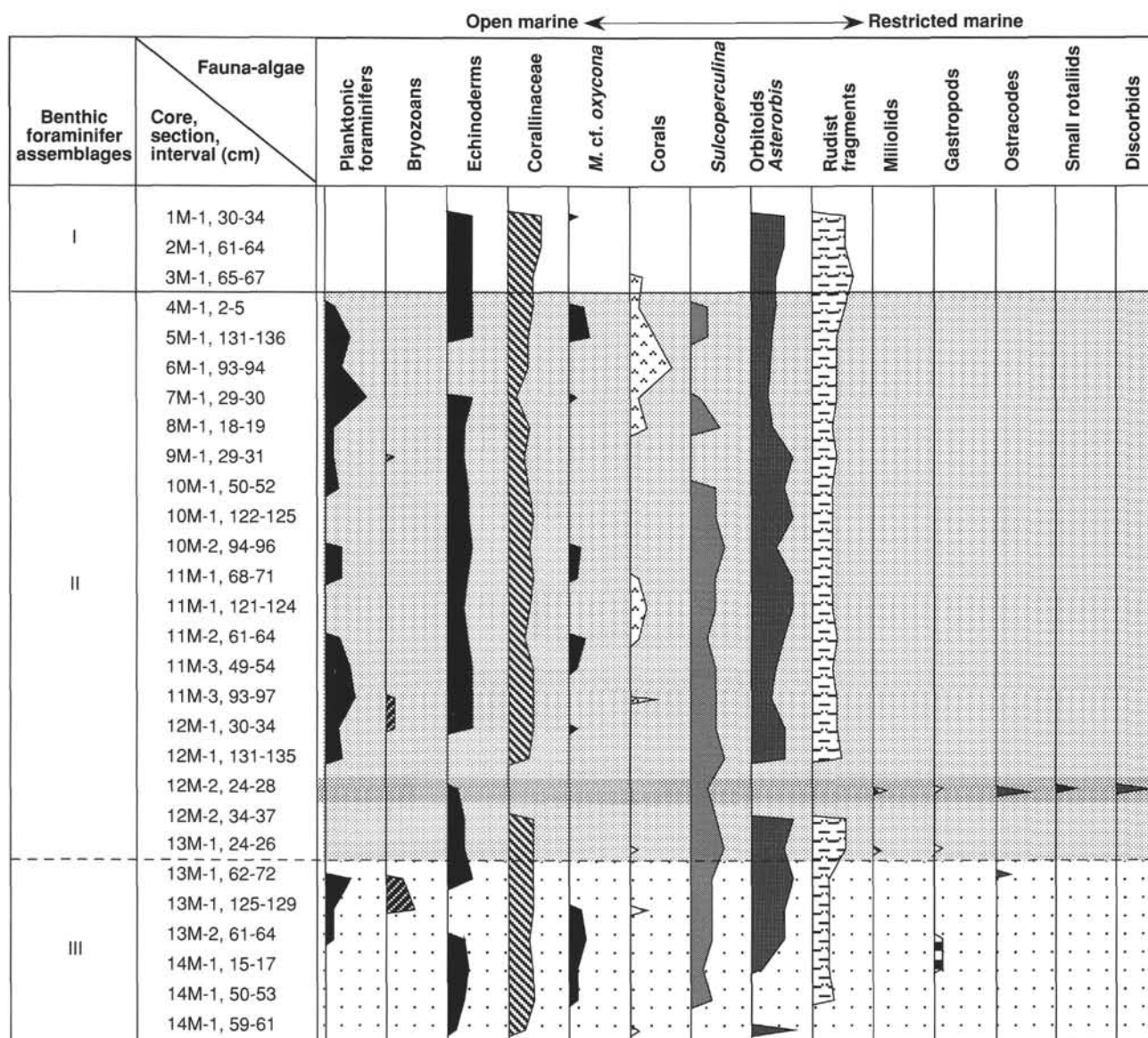


Figure 13. Distribution and relative abundance of selected foraminifers, algae, and megafossil fragments in Hole 875C arranged according to their paleoecologic affinities. Data are from observations of thin-section samples only. The stippled line corresponding to Sample 144-875C-12M-2, 24–28 cm, indicates a restricted marine assemblage.

### Planktonic Foraminifers

#### *Manganese-encrusted, Phosphatized Pelagic Limestone (Lithologic Unit I)*

Planktonic foraminifers occurring in the pelagic packstone, as with the calcareous nannofossils, demonstrate that this thin (a few centimeters) interval contains a complex and long geologic history. Planktonic foraminifers from the outer portion of the pelagic limestone are the best preserved and the most widespread. In Hole 875C, they belong to Zone P13 of late middle Eocene age, which was identified by the presence of *Turborotalia cerroazulensis*, *T. pomeroli*, *Orbulinoides beckmanni*, large globigerinathekids, *Globigerinatheka index*, *Morozovella lehneri*, *M. crassata*, *Acarinina rohri*, and *Truncorotaloides topilensis*. The second

assemblage observed below the outer manganese crust in Hole 875C—and occurring as the most external assemblage in Hole 876A—is attributable to Zone P11 of early middle Eocene age, based on the occurrence of *Morozovella aragonensis*, *Globigerinatheka index*, and *Turborotalia boweri* in the absence of *Turborotalia pomeroli*.

Older planktonic faunas occur in both Holes 875C and 876A in smaller slightly phosphatized areas to a few very phosphatized patches. They are attributed to Zones P8 of early Eocene and P4 of late Paleocene age. Species identifying Zone P8 are *Morozovella aragonensis*, *M. gracilis*, *M. crassata*, *Globigerinatheka senni*, *Acarinina pseudotopilensis*, and *Pseudohastigerina danvillensis* in the absence of globigerinathekids, hantkeninids, and turborotaliids. The Zone P4 assemblage includes *Morozovella velascoensis* gr., *M. pusilla* gr., *Acarinina intermedia*, and *Planorotalites*

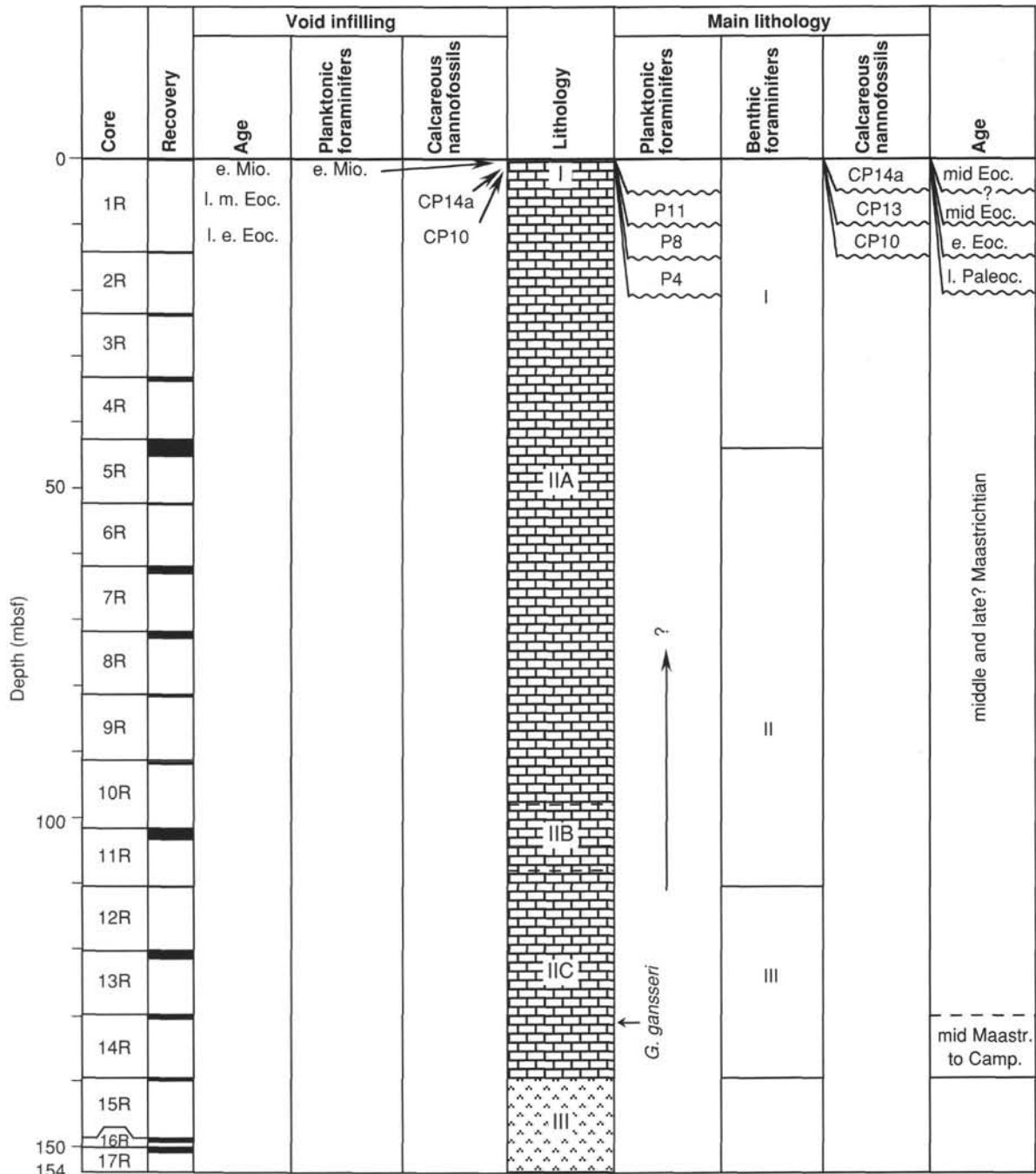


Figure 14. Biostratigraphy of Hole 876A, Wodejebato Guyot. Lithologic units and subunits are superimposed on the "Lithology" column.

*compressus*. In both Holes 875C and 876A, the planktonic foraminifers are rather densely packed, suggesting that they have been winnowed. Moreover, some fish remains occur in Hole 875C. The absence of a Zone P13 assemblage in Hole 876A is interpreted as resulting from the incomplete recovery of the pelagic limestone at this site.

Planktonic foraminifers in Sample 144-876A-1R-1, 43–48 cm, are also interpreted as belonging to the pelagic infilling of carbonate platform cavities. This sample yielded a well-preserved and rich planktonic fauna of early Miocene age. Identified species are *Globoquadrina binaiensis*, *Globigerinoides* sp. and representatives of the *Globoquadrina tripartita* group.

#### **Skeletal Grainstone and Packstone (Lithologic Unit II)**

The consistent presence of planktonic foraminifers throughout the skeletal grainstone and packstone is peculiar to Holes 875C and 876A, drilled on the outer perimeter ridge, in comparison with those sites drilled on the inner perimeter ridge of the guyot. This allows us to correlate the platform succession encountered on Wodejebato Guyot to the planktonic foraminifer zones and then directly date the succession.

The richest assemblage occurs in Core 144-875C-13M, in which several samples yielded *Gansserina gansseri*, *G. pettersi*,

*Rugoglobigerina rugosa*, *R. hexacamerata*, *Globotruncana arca*, *G. ventricosa*, *G. bulloides*, *G. orientalis*, and *Pseudotextularia elegans*. This assemblage is indicative of the *Gansserina gansseri* Zone of the middle Maastrichtian based on the co-occurrence of *G. ventricosa* and *G. bulloides* with the zonal marker, and in the absence of the index species of the youngest Maastrichtian zones, *Contusotruncana contusa* and *Racemiguembelina fructifera*, and *Abathomphalus mayaroensis*. Representatives of this assemblage are present upward through most of the sequence. However, planktonic faunas become progressively less diversified and abundant in some layers, thereby losing stratigraphic resolution. For the time being, the entire carbonate succession above Core 144-875C-13M can be dated as middle Maastrichtian, although extension into the late Maastrichtian cannot be ruled out. This age is in agreement with the record from DSDP Site 462 (Nauru Basin), where the larger foraminifer *Asterorbis-Sulcoperculina* assemblage was recovered from the middle Maastrichtian *G. gansseri* Zone (Premoli Silva and Brusa, 1981).

A relatively rich planktonic fauna of the *Gansserina gansseri* Zone occurs in Core 144-876A-14R, and elements of the same fauna occur through the top of the recovered sequence in Hole 876A. In this respect, the two holes drilled in the outer perimeter ridge of Wodejebato Guyot yielded an identical succession. Planktonic foraminifers are contained in the grainstone sequence to the base of Lithologic Unit II.

### Large Benthic Foraminifers

#### *Skeletal Grainstone and Packstone* (Lithologic Unit II)

The distribution of the microfauna and associated forms from the skeletal grainstone and packstone in Holes 875C and 876A was based on observations of hand specimens, thin-section samples, and isolated specimens recovered as cuttings from each section of a split core.

*Omphalocyclus macroporus* occurs in Sample 144-875C-1M-1, 34–40 cm, at the top of the carbonate sequence and may still be present in Sample 144-875C-13M-1, 125–129 cm. The most common larger foraminifers, which occur throughout the sequence studied down to Sample 144-875C-14M-1, 50–53 cm, are representatives of the genera *Asterorbis* and *Sulcoperculina*. The species identified are *Asterorbis havanensis*, *Sulcoperculina globosa*, *S. dickersoni*, and *S. vermunti*. Less common species are representatives of the genus *Lepidorbitoides*. The occurrence of *O. macroporus* and the whole foraminifer fauna indicate that most of the carbonate sequence in both holes has a Maastrichtian age. The association of Maastrichtian larger foraminifers with planktonic foraminifers of the *Gansserina gansseri* Zone of middle Maastrichtian age (see above) corroborates the age inferred for the other Wodejebato Guyot sites through comparison with the record of Site 462 in the Nauru Basin (Premoli Silva and Brusa, 1981).

A different assemblage is recorded in Sample 144-875C-14M-1, 59–61 cm: the fauna is rich in *Vaughanina*, *Pseudorbitoides*, and species of *Asterorbis* different from those recorded in the remainder of the carbonate sequence. No planktonic foraminifers or calcareous nannofossils are recorded from this sample. However, the same *Pseudorbitoides-Vaughanina* assemblage was recovered in Holes 874C and 877A, where it was directly dated by calcareous nannofossils as late Campanian in age. At DSDP Site 462, these two taxa were recorded within the *Globotruncanita calcarata* Zone of latest Campanian age (Premoli Silva and Brusa, 1981).

From the available record, no transition is recorded between the two assemblages mentioned above. Although biased by the

poor recovery, we suspect the presence of a hiatus within Core 144-875C-14M possibly spanning the lower Maastrichtian. This might also be inferred from Holes 873A and 874C, in which no transition between the *Sulcoperculina-Asterorbis* and *Pseudorbitoides-Vaughanina* assemblages was detected.

In Hole 876A, the carbonate succession is identical to Hole 875C, except that the samples studied did not yield the *Pseudorbitoides-Vaughanina* assemblage. This absence is interpreted as an interval of sediment missing because of poor recovery.

### Paleoenvironments of the Skeletal Grainstone and Packstone

#### Site 875

The skeletal grainstone and packstone sequence (Lithologic Unit II) recovered in Holes 875A (Core 144-875A-1R), 875B (Cores 144-875B-1R to -4R), and 875C (Cores 144-875C-1M to -14M) yielded common larger benthic foraminifers that are frequently associated with common mollusk fragments (mostly rudists), echinoderm fragments, fragments of Corallinaceae, and less frequent coral fragments. The distribution and relative abundance of these fossil groups is given in Figure 13.

Based on analyses of fossil remains directly from cores and from 28 thin-section samples, three assemblages can be differentiated within the skeletal grainstone and packstone (Lithologic Unit II). However, in Figure 13 only the results from thin-section analyses through Lithologic Unit II of Hole 875C are illustrated.

Three distinct fossil assemblages (Assemblages I to III) are differentiated within Lithologic Unit II.

#### Assemblage I

The interval from Section 144-875C-1M-1 to Sample 144-875C-3M-1, 65–67 cm, is characterized by the presence of abundant *Asterorbis* and by the absence of *Sulcoperculina* and planktonic foraminifers. The assemblage is dominated by abundant fragments of Corallinaceae, echinoderms, and rudists; coral fragments, however, are less abundant (Fig. 13). Other benthic foraminifer genera, including *Marssonella* sp. (e.g., in Sample 144-875C-1R-1, 30–34 cm), are rare. The association of these taxa indicates a normal marine environment on the edge of the platform; their test fragments comprise the sand.

#### Assemblage II

The interval from Samples 144-875C-4M-1, 2–5 cm, to -13M-1, 24–26 cm, is similar to Assemblage I, except that *Sulcoperculina* and/or planktonic foraminifers are common to abundant. Coral fragments and *Marssonella* are more frequent, although coral fragments become rare at the bottom of the interval.

At the base of the assemblage, a gastropod mudstone spans Interval 144-875C-12M-2, 15–33 cm. This mudstone contains a benthic foraminifer assemblage (in Sample 144-875C-12M-2, 24–26 cm) of restricted paleoenvironment, in contrast to the more open-marine conditions indicated by the presence of planktonic foraminifers in sands above and below this mudstone.

#### Assemblage III

The interval from Samples 144-875C-13M-1, 62–72 cm, to -14M-1, 59–61 cm, is defined by the occurrence of *Pseudorbitoides*, *Sulcoperculina*, and other species of *Asterorbis* different from those characterizing the overlying assemblages. The assemblage is quite similar to Assemblage II, but planktonic foraminifers are only recognized at the top (Samples 144-875C-13M-1, 62–72 cm, to -13M-1, 125–129 cm). The sediment within this interval is coarse sand that consists of skeletal fragments, many of which are probably reworked. Further study is necessary to

clarify which species are in place and which are reworked. Assemblage III reflects normal marine conditions.

Site 875 reflects a fore-slope environment and documents its evolution during the final submergence of the "atoll." The interval containing Assemblage III reveals progressive flooding of the former island and possible reworking of an older carbonate platform (perhaps Campanian or early Maastrichtian). This platform is questionably recognized at the bottom of the skeletal grainstone and packstone sequence (Interval 144-875C-14M-1, 0–65 cm), and in the pebbles and reworked larger benthic foraminifers occurring higher in the sequence. The presence of planktonic foraminifers at the top of Assemblage III and in Assemblage II indicates flooding of the platform edge. The paleowater depth increases upsection from probably a few meters in the lower part of Assemblage III to possibly more than 100 m at the top of Assemblage II. However, the dominance of sand throughout the skeletal grainstone and packstone sequence in Hole 875C implies that the fauna has been transported some distance from its normal environment.

#### Site 876

The 145-m sequence of skeletal grainstones and packstones (Lithologic Unit II) recovered in Holes 876A (Core 144-876A-1R to -15R) yielded common larger foraminifers that are associated with common mollusk fragments (mostly rudists), echinoderm fragments, fragments of Corallinaceae, and less frequent coral fragments. The distribution and relative abundance of these fossil groups is quite similar to those of Hole 875C, as shown in Figure 13.

Based on the analysis of fossils from thin-section samples and cores, the three distinct fossil assemblages (Assemblages I to III) that have been defined above for the skeletal grainstone and packstone sequence of Site 875 also occur within the limestone of Site 876. The distribution of these assemblages in Hole 876A is as follows: Assemblage I occurs from Sample 144-876A-1R-1, 17–21 cm, to Interval 144-876A-4R-1, 69–76 cm; Assemblage II occurs in the interval from Samples 144-876A-5R-1, 17–18 cm, to -11R-2, 43–46 cm; and Assemblage III occurs in the interval from Section 144-876A-12R-1 to Sample 144-876A-15R-1, 12 cm.

The paleoenvironmental interpretations of these assemblages made for Site 875 broadly apply also to Site 876. It should be noted, however, that (1) the packstone in the lower part of Assemblage II is thicker at Site 876 (Sections 144-876A-10R-1 to -11R-2); (2) no mudstone indicating a restricted marine influence was recovered at Site 875; and (3) Assemblage III is twice as thick at Site 876 than at Site 875. Moreover, comparison of Assemblage III at Sites 875 and 876 reveals some minor differences between them. At Site 875, planktonic foraminifers occur near the top of Assemblage III, but at Site 876 they occur near its observed base (Interval 144-876A-14R-1, 48–52 cm). The lower part of Assemblage III was not recovered in Hole 876A, perhaps suggesting that Assemblage III was even thicker than mentioned above.

### Summary

#### Site 875

The top of Hole 875C has a thin layer of manganese-encrusted, phosphatized limestone (Lithologic Unit I; 0.0–0.14 mbsf) that contains nannofossils and planktonic foraminifers in laminae, burrows, and clasts. Millimeter-scale biostratigraphy of this encrusted layer permits recognition of five phases of pelagic sedimentation: one in the late Paleocene, two in the early Eocene, and two in the middle Eocene. Each is bounded by disconformities. The pelagic infilling of a void within the underlying skeletal

grainstone/packstone sequence in Sample 144-875C-1R-1, 71–76 cm, contains nannofossils of late Eocene age.

The biostratigraphy of the underlying skeletal grainstone/packstone sequence (Lithologic Unit II; 0.14–126.0 mbsf) is based on planktonic and larger benthic foraminifers. *Omphalocyclus*, a benthic foraminifer genus restricted to the Maastrichtian, has its highest occurrence in Sample 144-875C-1M-1, 30–34 cm, constraining the age of the top of the limestone. A planktonic foraminifer assemblage including *Gansserina gansseri* occurs in Core 144-875C-13M, near the base of the limestone and allows assignment to the middle Maastrichtian. A Maastrichtian to Campanian age is indicated for the base of the limestone by the presence of the larger foraminifers *Pseudorbitoides* and *Vaughanina* in Sample 144-875C-14M-1, 59–61 cm. The skeletal grainstone/packstone sequence rests directly on basalt.

#### Site 876

In Hole 876A, 8 cm of manganese-encrusted, phosphatized limestone (Lithologic Unit I; 0–0.08 mbsf) was recovered. Nannofossil and planktonic foraminifer biostratigraphies indicate at least four phases of pelagic sedimentation: two in the middle Eocene, one in the early Eocene, and one in the late Paleocene. Each phase of sedimentation was separated by hiatuses.

Voids within the underlying skeletal grainstone/packstone sequence in Core 144-876A-1R have pelagic infillings that contain planktonic foraminifers and nannofossils of early and late middle Eocene (nannofossils) and early Miocene (foraminifers) ages.

The age of the top of the underlying skeletal grainstone/packstone sequence (Lithologic Unit II) is constrained by the occurrence in Sample 144-876A-1R-1, 17–21 cm, of *Asterorbis*, a benthic foraminifer not known higher than the Maastrichtian. A planktonic foraminifer assemblage including *Gansserina gansseri* occurs in Cores 144-876A-13R and -14R near the base of the skeletal grainstone/packstone sequence, dating this interval as middle to late Maastrichtian. The skeletal grainstone/packstone sequence rests directly on basalt.

### PALEOMAGNETISM

Sites 875 and 876, drilled on the outermost marginal buildup of Wodejebato Guyot, yielded primarily poorly cemented skeletal grainstones not suitable for shipboard paleomagnetic analysis. Magnetic susceptibility was not measured on the limestones because of the low recovery (average ca. 5%) and because previous measurements had shown the susceptibility record to be of limited use for correlation. Similarly, the small piece size and curated lengths of basement material from Holes 875C and 876A (0.87 and 2.62 m, respectively) were insufficient for meaningful susceptibility measurements.

The natural remanent magnetization (NRM) of limestones from Sites 875 and 876 was generally too weak ( $<1.0 \text{ mA}^{-1}$ ) to measure  $10 \text{ cm}^3$  discrete samples. Thus, more than 30 large pieces (up to  $250 \text{ cm}^3$ ) from the archive half of the split cores were subjected to alternating-field (AF) demagnetization and measured in discrete sample mode. Despite the enhanced magnetic moment of the larger pieces, several samples still proved to be below the effective noise level of the pass-through cryogenic magnetometer. The resulting magnetization directions included inclinations steeper than expected for the site and a tendency for declinations to cluster near  $180^\circ$  (Fig. 15A). We have not attempted any magnetostratigraphic interpretation. Samples with low NRM intensities (Fig. 15C) yield inconsistent results; however, results from the more strongly magnetized samples (e.g., Fig. 15B) suggest that shore-based measurements may yield reasonable results.

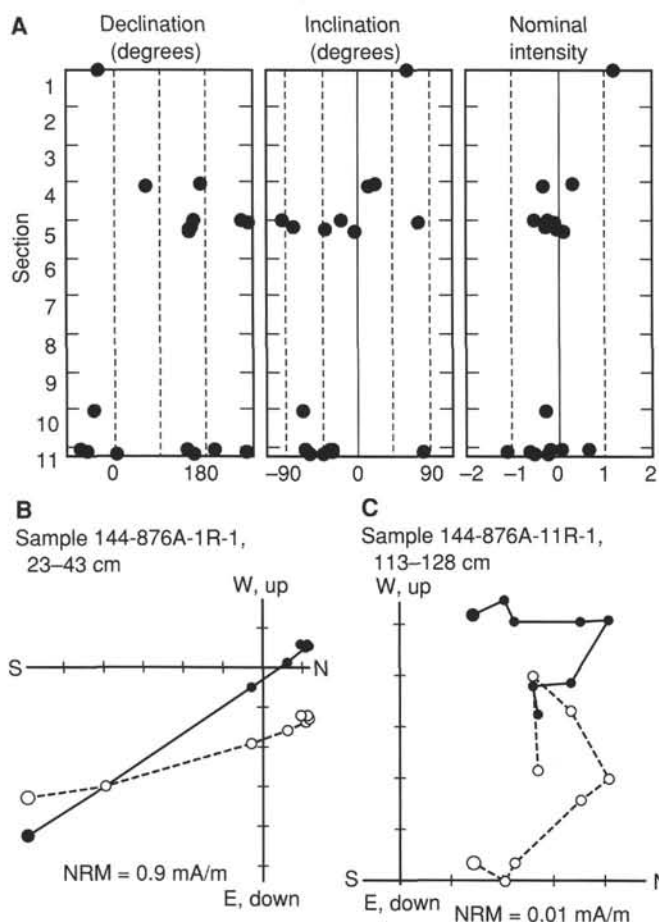


Figure 15. Results from limestone samples from Hole 876A. A. Declination, inclination, and intensity variations after demagnetization at 15 mT. Contrasting demagnetization behavior for relatively high magnetization (B) and very low magnetization (C) limestone samples are also illustrated. Closed circles represent horizontal components of the magnetization, and open circles represent vertical components. Demagnetization fields are 0, 2, 5, 7, 10, 12, 15, 17, and 20 mT. The low-stability component in Figure 15B is similar to the present field direction.

Three discrete samples of basalt and one discrete sample of volcanoclastic material from Sites 875 and 876 were demagnetized by applying an alternating magnetic field by means of the Schonstedt Model GSD-1 AC demagnetizer and measuring with the pass-through cryogenic magnetometer. The NRM intensities of the basalt samples ( $0.3\text{--}5.9\text{ Am}^{-1}$ ) are slightly lower than those measured from other sites on Wodejebato Guyot. The samples all had small to negligible low-stability components (Figs. 16–18) and a well-defined characteristic magnetization direction. Inclinations range from  $2^\circ$  to  $30^\circ$  (Table 6), compatible with a reversed magnetization acquired at low southern paleolatitudes. The average inclination derived from all 19 samples from Wodejebato Guyot ( $17^\circ \pm 7^\circ$ ) suggests a paleolatitude of about  $10^\circ\text{S}$ .

## INORGANIC GEOCHEMISTRY

### Interstitial Waters

No interstitial waters were taken from any cores in Holes 875C or 876A.

Sample 144-875A-15M-1, 24 cm

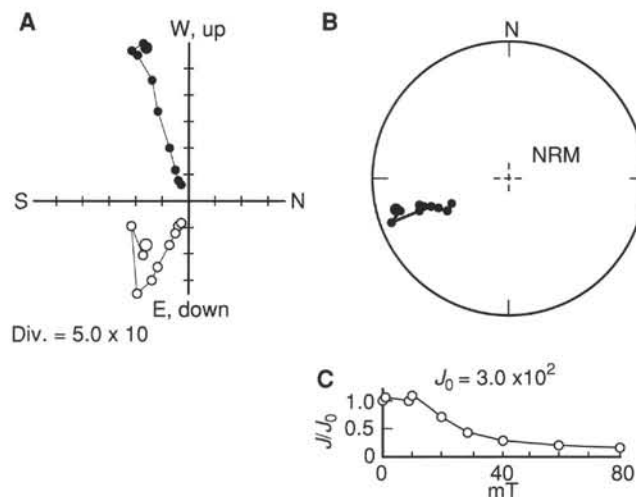


Figure 16. Alternating-field (AF) demagnetization results for basalt Sample 144-875-15M-1, 24 cm. Demagnetization fields are 0, 2.5, 10, 12.5, 15, 20, 29, 40, 60, and 80 mT. A. Orthogonal vector plot of progressive AF demagnetization. Closed circles represent horizontal components of the magnetization, and open circles represent vertical components. B. Stereonet plot of vector endpoints after progressive demagnetization. C. Variation of intensity after progressive AF demagnetization.

## Lithologic Data

Five limestone samples from Hole 875C and eight limestone samples from Hole 876A were analyzed according to the methods outlined in the “Explanatory Notes” chapter (this volume). Data are expressed as molar ratios to calcium for both minor and trace elements: ( $\text{Mg}/\text{Ca} \cdot 10^2$ ), ( $\text{Sr}/\text{Ca} \cdot 10^3$ ), ( $\text{F}/\text{Ca} \cdot 10^3$ ), ( $\text{PO}_4/\text{Ca} \cdot 10^3$ ), ( $\text{SiO}_2/\text{Ca} \cdot 10^3$ ), ( $\text{Fe}/\text{Ca} \cdot 10^3$ ), and ( $\text{Mn}/\text{Ca} \cdot 10^4$ ). Shipboard rock sample data from Sites 875 and 876 are presented in Table 7.

### Magnesium, Strontium, Fluoride, and Phosphate

Magnesium/calcium and strontium/calcium ratios in rock samples from Holes 875C and 876A range from 0.65 to 1.95 and from 0.27 to 1.28, respectively, and are consistent with the alteration of metastable aragonite and high magnesian calcite to more stable low-magnesian calcite ( $<3\text{ mM Mg}$ ) (Fig. 19). Fluoride/calcium and phosphate/calcium ratios in rock samples from Holes 875C and 876A range from 0.17 to 2.30 and from 0.35 to 19.88, respectively, and are indicative of the presence of some form of fluorapatite (Fig. 19).

### Silica, Iron, and Manganese

Silica/calcium ratios in rock samples from Hole 877A range from 0 to 1.75. These low ratios are consistent with relatively pure carbonate rocks, poor in metastable silica. Iron/calcium and manganese/calcium ratios range from 0.14 to 8.43 and from 0.02 to 15.61, respectively (Fig. 19).

## Summary

Sites 875 and 876 data are consistent with (1) alteration of metastable aragonite and high-magnesian calcite to more stable low-magnesian calcite in limestones and (2) the probable presence of some form of fluorapatite in limestones.

Sample 144-876A-16R-1, 6 cm

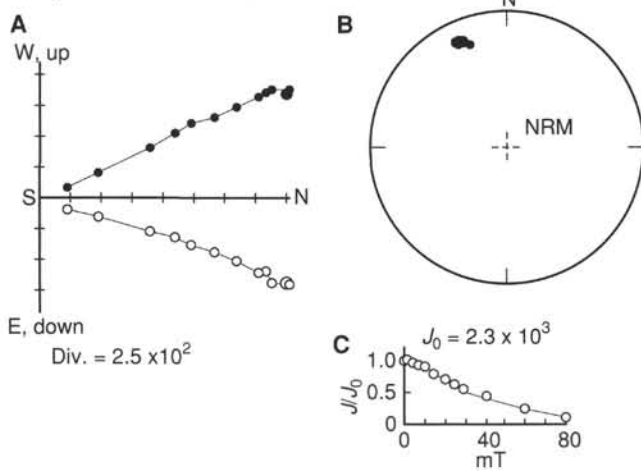


Figure 17. Alternating-field (AF) demagnetization results for basalt Sample 144-876A-16R-1, 6 cm. Demagnetization fields are 0, 2.5, 5, 7.5, 10, 15, 20, 25, 29, 40, 60, and 80 mT. Other plot conventions are identical to Figure 16.

Sample 144-876A-17R-1, 91 cm

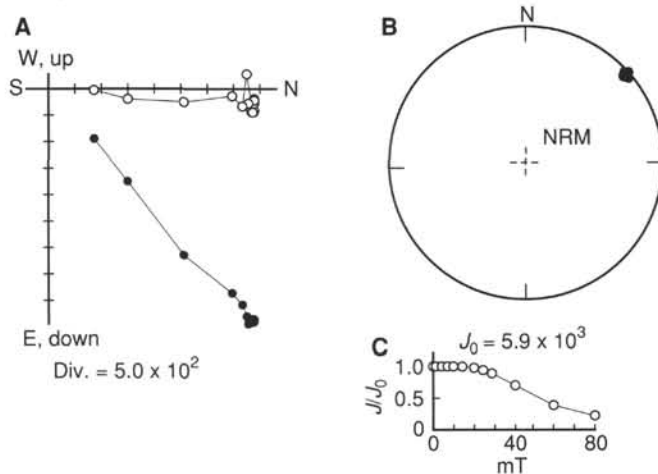


Figure 18. Alternating-field (AF) demagnetization results for basalt Sample 144-876A-17R-1, 91 cm. Demagnetization fields are 0, 2.5, 5, 7.5, 10, 15, 20, 25, 29, 40, and 60 mT. Other plot conventions are identical to Figure 16.

Table 6. Results of demagnetization of discrete samples, Holes 875A and 876A.

Core, section, interval (cm)	Lithology	Inclination (degrees)
144-875A-		
15M-1, 24-26	Basalt	+30
16R-1, 6-8	Basalt	+14.0
144-876A-		
17R-1, 26-28	Volcaniclastic	+13.3
17R-1, 91-93	Basalt	+1.8

## ORGANIC GEOCHEMISTRY

### Introduction

Sites 875 and 876 were drilled on the outer perimeter ridge of Wodejebato Guyot. The type of rocks encountered at the sites included (from top to bottom): manganese-encrusted limestone

Table 7. Lithologic geochemical data, Holes 875C and 876A.

Core, section, interval (cm)	Depth	Mg/Ca ( $\cdot 10^2$ )	Sr/Ca ( $\cdot 10^3$ )	F/Ca ( $\cdot 10^3$ )	PO <sub>4</sub> /Ca ( $\cdot 10^3$ )	Fe/Ca ( $\cdot 10^3$ )	Mn/Ca ( $\cdot 10^4$ )
144-875C-							
1M-1, 20	0.20	1.34	1.28	0.43	1.37	6.70	0.43
6M-1, 43	46.83	1.49	0.29	0.17	0.45	2.20	0.17
11M-3, 32	97.99	1.54	0.33	0.02	0.86	4.00	0.02
12M-2, 11	105.92	1.95	0.34	0.29	0.86	4.20	0.29
14M-1, 80-83	124.43	1.20	0.51	0.65	0.32	1.50	0.67
144-876A-							
1R-i, 36-42	0.36	0.72	1.21	2.30	15.09	0.37	2.07
1R-ii, 36-42	0.36	0.98	1.16	1.56	19.88	8.43	15.6
5R-2i, 28-33	44.78	1.60	0.32	0.34	0.53	0.23	0.33
5R-2ii, 28-33	44.78	0.88	1.08	0.51	0.35	0.18	0.37
5R-2, 44-50	44.94	1.48	0.30	0.20	0.39	0.16	0.21
11R-1, 131-135	102.11	1.49	0.27	0.15	0.36	0.14	0.33
13R-1, 25-30	120.35	1.67	0.39	0.56	1.37	0.21	0.34
13R-1, 34-37	120.44	0.65	1.18	0.48	0.44	0.33	0.21

(Lithologic Unit I; see "Lithostratigraphy" section, this chapter), skeletal grainstone and packstone (Unit II), and basalt (Unit III). As the lithologies of the two sites are very similar, the Shipboard Scientific Party decided to include both sites in the same chapter.

The analytical program for Holes 875A and 876A included chemical analyses of 40 samples of limestone. We analyzed 17 samples from Hole 875A and 23 samples from Hole 876A for inorganic carbon (IC). Out of these, 31 samples were analyzed for total organic carbon (TOC), nitrogen (N), and total sulfur (TS). None of the samples contained enough organic matter for pyrolysis analysis. No headspace gas analyses were performed at the sites. The procedures used for the analytical program are described in the "Organic Geochemistry" section, "Explanatory Notes" chapter (this volume).

### Carbonate Carbon

Inorganic carbon (IC) content was measured with the Coulometrics carbon dioxide coulometer and reported as weight% calcium carbonate. Sampling was performed in a way to obtain representative material with regard to both lithotypes and depth. In Hole 875A, microsamples were obtained from the chips used for physical properties measurements by hand drilling with a standard 5-mm drill bit. In Hole 876A, separate samples were taken for carbonate analysis and subjected to the same sampling procedure as in Hole 875A. No sampling was performed on the basalt. Results of the inorganic carbon analyses are given in Table 8. Calcium carbonate data are shown in Figure 20.

Carbonate content was very high in all samples except the partly manganese-encrusted skeletal grainstone in Core 144-876A-1R-1. Average carbonate content in Lithologic Unit II was 99.0% for Hole 875A and 97.8% for Hole 876A. No significant changes were seen either with depth or with lithotypes in the two holes.

### Organic Carbon and Total Sulfur

The content of total carbon (TC), nitrogen (N), and total sulfur (TS) was determined using the Carlo-Erba Model NA1500 elemental analyzer. Total organic carbon (TOC) values were calculated from the difference between TC and IC. Detection limits for TOC, N, and TS are 0.1%, 0.02%, and 0.02%, respectively. Analyses were performed on the 31 samples used for carbonate carbon determinations. The results of the TOC, N, and TS analyses are given in Table 8.

Very low TOC values were found in the skeletal grainstone and skeletal packstone from Holes 875A and 876A. Organic

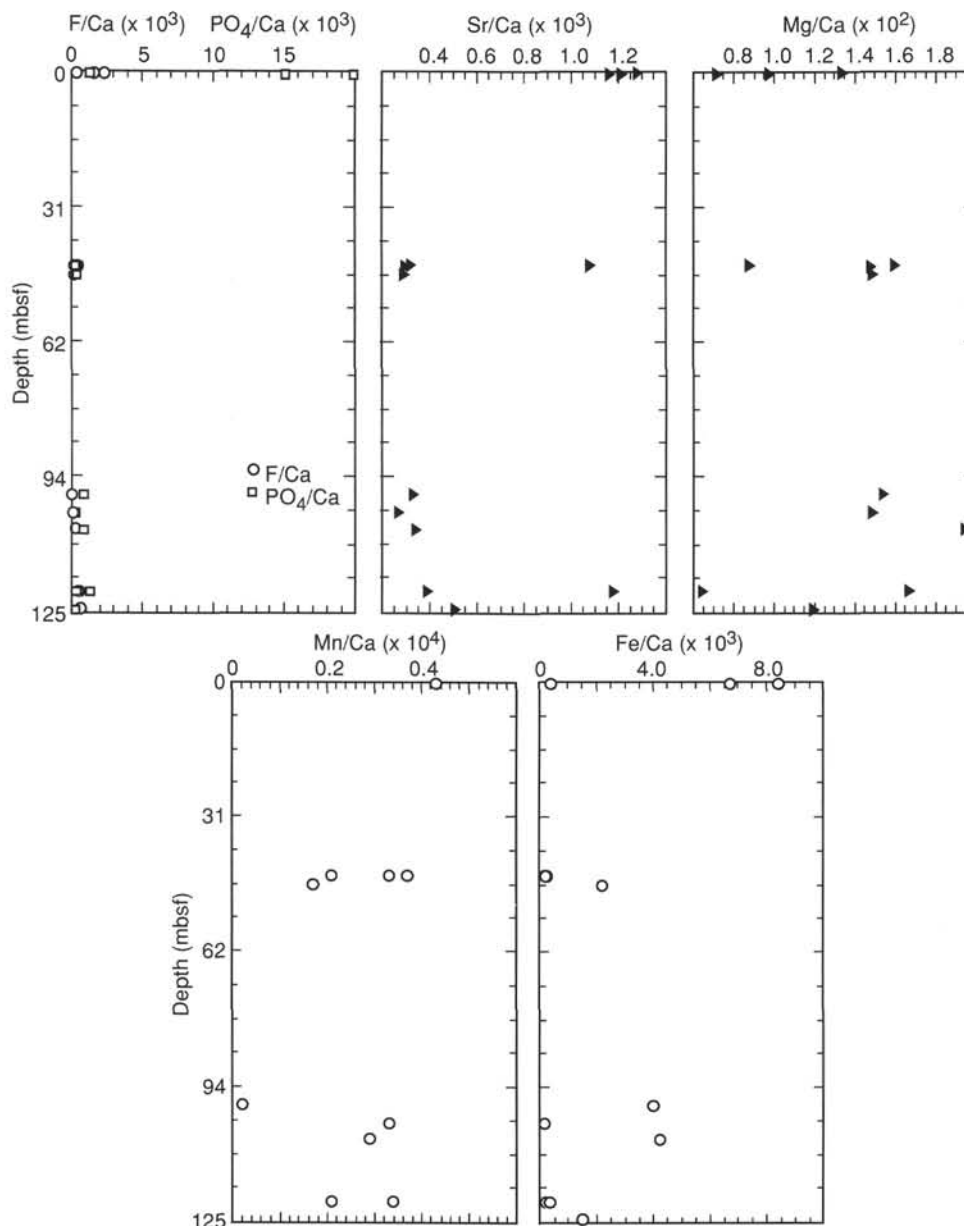


Figure 19. Elemental abundances of rock samples vs. depth, Holes 875C and 876A. Abundances are expressed as a molar ratio with respect to calcium.

carbon content reached values of 0.23% in the manganese-enriched skeletal grainstone in Core 144-876A-1R-1 and was below 0.2% in the remaining samples (average TOC = 0.06% for both holes). Nitrogen and sulfur concentrations were below the detection limit in all samples investigated.

#### Organic Matter Type and Thermal Maturation Level

Because of the extremely low TOC concentration in Holes 875A and 876A, no attempts were made to determine type or thermal maturation of organic matter.

#### Interpretation of Organic Facies and Depositional Environments

The only major depositional environment represented in Holes 875A and 876A was shallow-water, open-marine in nature. In this

environment, the preservation of organic matter was extremely poor. TOC values below 0.25% and TS values below the detection limit in all samples indicate deposition under oxic conditions with very low preservation potential for organic matter. Most of the organic matter was probably of marine origin, but no visual inspection of organic matter residues was performed to substantiate this assumption.

## IGNEOUS PETROLOGY

### Introduction

Sites 875 and 876 were located on the outer perimeter ridge near the northern edge of Wodejebato Guyot. Holes 875C and 876A passed directly from limestone into basaltic basement with little or no indication of an intervening weathering horizon. This result is in marked contrast to the thick clay weathering profiles

**Table 8. Results of geochemical analyses, Holes 875C and 876A.**

Core, section, interval (cm)	Depth (mbsf)	IC (wt%)	CaCO <sub>3</sub> (wt%)	TC (wt%)	TOC (wt%)	N (wt%)	TS (wt%)	Lithology
144-875C-								
1M-1, 63-65	0.65	11.98	99.8	11.99	0.01	0	0	Skeletal grainstone
2M-1, 119-127	10.77	12.01	100.0	ND	ND	ND	ND	Skeletal grainstone
3M-1, 37-40	17.90	11.86	98.8	11.95	0.09	0	0	Skeletal grainstone
4M-1, 55-63	27.73	11.90	99.1	11.98	0.08	0	0	Skeletal grainstone
6M-1, 101-106	47.46	11.91	99.2	ND	ND	ND	ND	Skeletal grainstone
7M-1, 40-48	56.48	11.93	99.4	ND	ND	ND	ND	Skeletal grainstone
8M-1, 31-35	66.05	11.92	99.3	ND	ND	ND	ND	Skeletal grainstone
9M-1, 44-50	75.80	11.88	99.0	11.95	0.07	0	0	Skeletal grainstone
10M-2, 70-74	87.24	11.87	98.9	ND	ND	ND	ND	Skeletal grainstone
11M-2, 106-113	97.30	11.91	99.2	ND	ND	ND	ND	Skeletal grainstone
11M-3, 86-92	98.59	11.87	98.9	11.98	0.11	0	0	Skeletal grainstone
12M-1, 125-130	105.60	11.85	98.7	ND	ND	ND	ND	Skeletal packstone
12M-1, 8-20	106.00	11.66	97.1	ND	ND	ND	ND	Skeletal packstone
13M-1, 24-26	114.16	11.95	99.5	11.97	0.02	0	0	Skeletal grainstone
13M-1, 107-110	115.00	11.88	99.0	11.90	0.02	0	0	Skeletal grainstone
13M-2, 90-93	116.13	11.89	99.0	ND	ND	ND	ND	Skeletal grainstone
14M-1, 15-17	123.77	11.86	98.8	11.86	0	0	0	Skeletal grainstone
144-876A-								
1R-1, 8-16	0.16	8.38	69.8	8.59	0.21	0	0	Skeletal grainstone
1R-1, 23-43	0.43	9.56	79.6	9.75	0.19	0	0	Skeletal grainstone
1R-1, 49-54	0.54	9.19	76.6	9.19	0	0	0	Skeletal grainstone
1R-1, 66-71	0.71	11.00	91.6	11.23	0.23	0	0	Skeletal grainstone
2R-1, 35-39	14.59	11.68	97.3	11.75	0.07	0	0	Skeletal grainstone
3R-1, 75-83	24.53	11.73	97.7	11.62	0	0	0	Skeletal grainstone
4R-1, 90-94	34.24	11.76	98.0	11.80	0.04	0	0	Skeletal grainstone
5R-1, 74-76	43.76	11.73	97.7	11.60	0	0	0	Skeletal grainstone
5R-2, 76-86	45.36	11.74	97.8	11.74	0	0.01	0	Skeletal grainstone
5R-3, 40-45	46.45	11.60	96.6	11.70	0.10	0	0	Skeletal grainstone
6R-1, 0-4	52.64	11.69	97.4	11.71	0.02	0.02	0	Skeletal grainstone
7R-1, 86-91	63.11	11.66	97.1	11.74	0.08	0	0	Skeletal grainstone
8R-1, 18-21	72.11	11.68	97.3	11.84	0.16	0	0	Skeletal grainstone
9R-1, 24-30	81.80	11.65	97.0	11.74	0.09	0	0.01	Skeletal grainstone
10R-1, 19-26	91.46	11.84	98.6	11.80	0	0	0	Skeletal grainstone
11R-1, 23-28	101.08	11.70	97.5	11.76	0.06	0	0	Skeletal grainstone
11R-2, 23-33	102.53	11.92	99.3	11.98	0.06	0	0	Skeletal grainstone
12R-1	110.50	11.74	97.8	11.88	0.12	0	0	Skeletal packstone
13R-1	120.10	11.73	97.7	11.74	0.01	0	0	Skeletal grainstone
13R-1, 37-40	120.50	11.91	99.2	12.06	0.15	0	0	Skeletal grainstone
14R-1	129.80	11.94	99.5	11.86	0	0	0	Skeletal grainstone
14R-1, 66-76	130.56	11.60	96.6	11.69	0.09	0	0	Skeletal grainstone
15R-1	139.40	11.78	98.1	11.87	0.09	0	0	Skeletal grainstone

Notes: IC = inorganic carbon, CaCO<sub>3</sub> = carbonate carbon calculated as calcium carbonate, TC = total carbon, TOC = total organic carbon, N = nitrogen, and TS = total sulfur. ND = no determination. All numbers are in weight percent.

encountered at Sites 873, 874, and 877, which are nearer to the center of the geyot.

### Hole 875C

In Hole 875C, limestones near the base of Lithologic Subunit IIC become increasingly iron stained through Interval 144-875C-14M-1, 44-65 cm, and a few small basalt fragments are incorporated in Interval 144-875C-14M-1, 62-65 cm (see "Lithostratigraphy" section, this chapter). Below this interval, the hole passed into basaltic lava of Lithologic Unit III at 124.3 mbsf. Approximately 85 cm of basalt, all from a single flow, was recovered before the hole was terminated at 133.0 mbsf.

The basalt pieces recovered in Hole 875C are predominantly gray in color, with areas of brownish or greenish discoloration, and they are somewhat friable to the touch. These characteristics reflect a significant degree of alteration. The basalt is highly vesicular with numerous, relatively coarse-grained (0.5-2 mm) plagioclase laths and prisms visible in hand specimen. This fabric strongly resembles the relict basaltic fabric preserved in the upper part of the claystone layer of Hole 874B (Sections 144-874B-21R-1, 2 cm, through -22R-2, 77 cm). This similarity suggests that the same flow, or a series of closely related flows, is present at both sites.

The primary mineralogy of the Site 875 basalt is dominated by dense clusters of relatively coarse-grained plagioclase laths and prisms; much of the plagioclase has been altered to cloudy,

colorless clay. Olivine was present both as phenocrysts (~15%) and in the groundmass (~5%); it is now completely altered to green-brown clay. As with the great majority of lavas from the other Wodejebato Guyot sites, well-formed magnetite grains make up a significant proportion of the lava and appear to have formed fairly early in the crystallization sequence. Based on this observation and on the alkalic nature of many of the other lavas recovered, we tentatively identify this as an alkali olivine basalt.

An interesting feature of the Site 875 basalt is the presence in the uppermost pieces (Interval 144-875C-14M-1, 68-76 cm) of relatively abundant (1%-2%) secondary pyrite. The pyrite appears quite fresh and is concentrated along fine fractures in the basalt and around the margins of many vesicles. Its presence suggests that the reducing conditions, which prevailed during the transition from subaerial to marine conditions at Sites 874 and 877 (see "Lithostratigraphy" section, "Site 874" chapter, this volume), were also present at Site 875.

### Hole 876A

In Hole 876A, several altered basalt pebbles were recovered at the limestone-basalt interface near 139.5 mbsf (Interval 144-876A-15R-1, 12-18 cm). Some of these are enclosed by a lithified limestone matrix (see "Lithostratigraphy" section, this chapter). The pebbles are subangular to subrounded in shape and 1-2 cm in size. They record a moderately high-energy erosional environment, presumably close to sea level, before the onset of marine

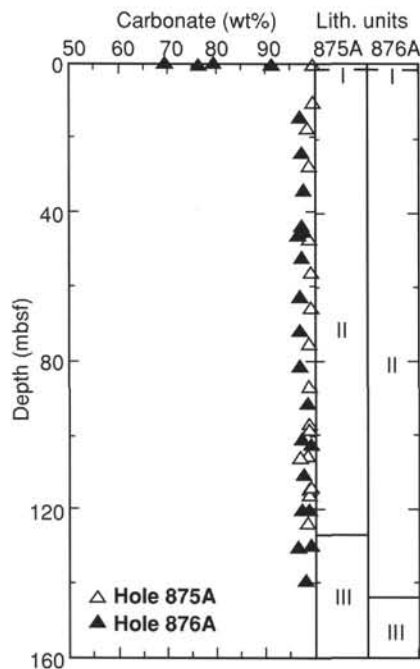


Figure 20. Carbonate content of sediments in Holes 875C and 876A, calculated as calcium carbonate. Also shown are the major lithologic units, as given in the "Lithostratigraphy" section (this chapter).

sedimentation. Immediately beneath the pebble interval, basaltic lavas were encountered at 139.5 mbsf (Sections 144-876A-15R-1, 18 cm, through -17R-1, 103 cm); Hole 876A terminated at 154.0 mbsf. The basaltic interval drilled was 14.5 m and the recovery approximately 2.2 m (~15%).

The uppermost basalts (Interval 144-876A-15R-1, 68–76 cm) are brownish in color and appear to have undergone a relatively brief period of oxidative weathering, in contrast to the extensive weathering profiles at Sites 873 and 874 and to the reducing conditions that characterize this part of the section at Site 875.

Three texturally distinct basalt flow units (Units 1, 3, and 4) and one volcanic breccia (designated as Unit 2) were identified (Table 9). Unit 2 is most likely the brecciated flow top of Unit 3. Unit 1 (Sections 144-876A-15R-1, 18 cm, through -16R-1, 35 cm) and Unit 3 (Interval 144-876A-17R-1, 40–96 cm) are very fine-grained alkali basalts with sparse microphenocrysts of clinopyroxene and olivine. They are moderately altered, as reflected in the brownish and greenish discoloration of the matrix. In thin section, both basalts have intersertal to pilotaxitic textures, dominated by plagioclase, with interstitial clinopyroxene and relatively abundant, well-crystallized magnetite. In the sections examined, the plagioclase of Unit 1 is completely altered to colorless

or light brown clay; in Unit 3, however, the plagioclase remains remarkably unaltered. Both samples contain 5%–10% interstitial green clay, some of which appears to have replaced original groundmass olivine.

The volcanic breccia of Unit 2 (Sections 144-876A-16R-1, 35 cm, through -17R-1, 40 cm) has a recovered thickness of about 1 m. The breccia is friable, especially when it has dried out, reflecting extensive alteration to clay, and it has been oxidized to predominantly dark red colors. Despite the alteration, the primary structure of the breccia is clearly preserved. The clasts are subangular to subrounded basalt fragments that appear in hand specimen to be quite variable in texture and vesicularity. In thin section, they are almost opaque, owing to the pervasive alteration; a very fine-grained, well-crystallized, pilotaxitic to intersertal texture can still be discerned, however. This texture strongly resembles that of underlying Unit 3. Between the clasts, about half the void space appears to have contained finely broken basalt fragments that have since been altered to brown clay. The remaining void space, now filled by an equigranular mosaic of well-crystallized calcite and the zeolite, chabazite, appears to have originally been empty. These characteristics suggest that the Site 876 breccia formed as the top of the underlying lava flow. It is quite distinct from the hyaloclastic breccias of Site 873.

Unit 4, a relatively coarse-grained alkali basalt, is represented by a single piece of core (Interval 144-876A-17R-1, 96–103 cm). It is a plagioclase-microphyric lava with up to 20% visible laths and prisms and glomerocrysts of plagioclase, altered to white clay or zeolites, in a dark, microcrystalline matrix. Its mineralogy is dominated by plagioclase, which forms glomerophyric aggregates of relatively large (~1 mm) laths, and by striking glomerocrysts of smaller (0.2–0.5 mm), anhedral titanite grains with minor (altered) olivine.

### Summary

Holes 875C and 876A ended in alkalic basalt flows, which share the dominant mineralogic characteristics of all flows recovered from Wodejebato Guyot. Plagioclase is abundant, olivine is relatively scarce, and xenocrysts or glomerocrysts of titaniferous clinopyroxene are ubiquitous, although not usually abundant. We interpret the mineralogy of these flows as consistent, with only a slight to moderate degree of undersaturation, equivalent to lavas of the alkalic cap stage of Hawaiian volcanism and in contrast to the more strongly undersaturated lavas recovered from Limalok Guyot (Site 871).

All four of the lavas recovered at these two sites appear to have formed relatively thin (less than a few meters) massive flows and one has a brecciated flow top. They most likely represent a subaerial sequence. In contrast to the more central sites on Wodejebato Guyot, these outer perimeter ridge sites do not record significant weathering intervals before the onset of marine conditions. At Site 875, the uppermost basalts were subject to reducing conditions before or coincident with the onset of marine sedimentation; at Site 876, however, oxidative weathering affected the

Table 9. Summary of igneous units, Holes 875C and 876A.

Unit	Cores	Description
1	Sections 144-875C-14M-1, 65 cm, to 15M-1, 77 cm	Highly vesicular, altered basalt
1	Sections 144-876A-15R-1, 18 cm, to 16R-1, 35 cm	Very fine-grained, aphyric alkali basalt
2	Sections 144-876A-16R-1, 35 cm, to 17R-1, 40cm	Volcanic breccia (flow top to Unit 3?)
3	Interval 144-876A-17R-1, 40–96 cm	Sparsely olivine and clinopyroxene phyric alkali basalt
4	Interval 144-876A-17R-1, 96–103 cm	Plagioclase microphyric, medium-grained alkali basalt

uppermost basalts to a limited degree. A pebble conglomerate interval overlying the basalts provides the only evidence for even a moderate energy environment at this time.

## PHYSICAL PROPERTIES

### Introduction

The objectives of the physical properties measurement program at Sites 875 and 876 were (1) to measure standard shipboard physical properties and (2) to identify downhole geotechnical units. Standard index properties measurements and Hamilton Frame compressional-wave velocities, measured using sample cubes of limestone and basalt, comprised the major part of the shipboard analyses ("Explanatory Notes" chapter, this volume) at Site 875.

Hard-rock cores were obtained in Holes 875A and 875B using the rotary core barrel (RCB), but recovery was very poor; therefore, samples were not tested for physical properties. Hole 875C was drilled using the motor-driven core barrel (MDCB). Core recovery in Hole 875C was poor; the best recovery (35%) was in the lowermost 40 m of limestone. At Site 876, a single RCB hole was drilled that recovered 140 m of limestone.

Samples recovered in Holes 875C and 876A consist of limestones (Hole 875C, 0–126 mbsf; Hole 876A, 0–145.5 mbsf) and basalt (Hole 875C, 126.0–133.0 mbsf; Hole 876A, 145.5–154.0 mbsf). The limestones consist of neritic, white, highly porous, coarse sand-sized, skeletal grainstone of Maastrichtian age. The neritic limestone is capped by a very thin pelagic packstone of early and middle Eocene age encrusted with manganese oxide. A thin mudstone/packstone horizon is seen between 105.5 and 113.9 mbsf in Hole 875C. Test data are given in Table 10, and the index property data for Holes 875C and 876A are shown in Figures 21 and 22.

Table 10. Index properties data, Holes 875C and 876A.

Core, section, interval (cm)	Depth (mbsf)	Wet-bulk density (g/cm <sup>3</sup> )	Dry-bulk density (g/cm <sup>3</sup> )	Grain density (g/cm <sup>3</sup> )	Porosity (%)	Water content (% dry wt)	Void ratio
144-875C-							
1M-1, 63-65	0.63	2.18	1.75	2.76	41.3	19.4	0.70
2M-1, 119-121	10.69	2.17	1.75	2.78	40.6	19.2	0.68
3M-1, 37-39	17.87	2.23	1.76	2.80	46.4	21.3	0.87
3M-1, 65-67	18.15	2.24	1.86	2.77	37.1	17.0	0.59
4M-1, 55-57	27.65	2.21	1.83	2.75	37.4	17.3	0.60
5M-1, 119-121	37.99	2.36	1.95	3.19	40.1	17.4	0.67
6M-1, 101-103	47.41	2.37	1.94	2.72	41.7	18.0	0.72
7M-1, 40-42	56.40	2.24	1.83	2.72	40.9	18.7	0.69
8M-1, 31-33	66.01	2.19	1.78	2.75	39.7	18.6	0.66
9M-1, 44-46	75.74	2.34	2.01	2.72	31.6	13.9	0.46
10M-2, 70-72	87.20	2.58	2.25	2.75	32.1	12.7	0.47
11M-2, 106-108	97.23	2.32	1.90	2.85	40.5	17.9	0.68
11M-3, 86-88	98.53	2.21	1.84	2.77	35.6	16.5	0.55
12M-1, 125-127	105.55	2.64	2.49	2.81	15.4	5.9	0.18
12M-2, 8-10	105.88	2.58	2.41	2.80	16.8	6.7	0.20
13M-1, 24-26	114.14	2.33	1.95	2.76	37.4	16.5	0.60
13M-1, 107-109	114.97	2.46	2.19	2.80	26.0	10.8	0.35
13M-2, 90-92	116.10	2.31	1.98	2.78	32.6	14.4	0.48
14M-1, 15-17	123.75	2.59	2.40	2.76	19.1	7.6	0.24
14M-1, 66-68	124.26	2.35	1.98	3.19	35.8	15.6	0.56
15M-1, 55-57	127.15	2.37	2.08	3.34	28.5	12.3	0.40
144-876A-							
1R-1, 53-55	0.53	2.60	2.36	2.86	24.0	10.4	0.32
2R-1, 1-3	14.21	2.15	1.69	2.82	44.5	26.9	0.80
3R-1, 76-77	24.46	2.56	2.29	2.82	26.2	11.7	0.36
4R-1, 102-103	34.32	2.18	1.72	2.76	44.8	26.7	0.81
5R-1, 46-48	43.46	2.02	1.54	2.80	46.7	31.1	0.88
5R-3, 18-20	46.18	2.09	1.61	2.83	46.9	29.8	0.88
7R-1, 77-79	62.97	2.03	1.55	2.78	47.2	31.2	0.89
8R-1, 72-74	72.62	2.15	1.75	2.74	39.2	23.0	0.64
9R-1, 24-26	81.74	2.20	1.78	2.76	41.2	23.7	0.70
10R-1, 16-19	91.36	2.62	2.55	2.68	6.9	2.8	0.07
11R-1, 23-25	101.03	2.91	2.86	2.73	4.4	1.6	0.05
11R-1, 115-117	101.95	2.78	2.72	2.74	6.0	2.3	0.06
13R-1, 37-39	120.47	2.34	2.03	2.80	30.6	15.5	0.44
14R-1, 66-68	130.46	2.21	1.81	2.78	39.5	22.4	0.65
15R-1, 73-75	140.13	2.58	2.36	3.06	22.0	9.6	0.28
16R-1, 6-8	147.86	2.87	2.73	3.04	13.4	5.0	0.15
16R-1, 29-31	148.09	2.41	2.07	3.34	33.2	16.5	0.50
17R-1, 26-28	150.26	2.47	2.17	3.32	29.6	14.0	0.42
17R-1, 69-71	150.69	2.97	2.91	2.99	6.0	2.1	0.06

## Physical Properties Units

### Limestone

The limestones may be tentatively divided into three geotechnical subunits: Subunit 1A (Hole 875C, 0–105.5 mbsf; Hole 876A, 0–98 mbsf), which is equivalent to Lithologic Subunit IIA; Subunit 1B (Hole 875C, 105.5–113.9 mbsf; Hole 876A, 98.0–108 mbsf), which is equivalent to Lithologic Subunit IIB; and Subunit 1C (Hole 875C, 113.9–126.0 mbsf; Hole 876A, 108.0–145.5 mbsf), which is equivalent to Lithologic Subunit IIC. Geotechnical Subunits 1A and 1C have essentially the same values of geotechnical properties, whereas Subunit 1B has notably higher wet- and dry-bulk densities, lower water content, and lower porosity than either Subunits 1A or 1C (Figs. 21–22). Porosity values are generally higher in the limestones because of their coarse-grained, open, skeletal structure, and lower in slightly weathered basalt.

Dry-bulk density values in Subunits 1A and 1C range from 1.54 to 2.36 g/cm<sup>3</sup> in both holes, with a mean of 1.91 g/cm<sup>3</sup>. Porosity values for Subunits 1A and 1C range from 18% to 46% in both holes, with a mean of 35.6%. Dry-bulk density values for Subunit 1B range from 2.41 to 2.86 g/cm<sup>3</sup>, with a mean of 2.49 g/cm<sup>3</sup>. Porosity values for Subunit 1B range from 4% to 16%, with a mean of 10.2%. Grain density is reasonably constant throughout the limestones, with an overall mean of 2.8 g/cm<sup>3</sup>, the exception being a single high value of 3.19 g/cm<sup>3</sup> at a depth of 38 mbsf in Hole 875C.

The plot of compressional wave velocity vs. sub-bottom depth (Fig. 23) reveals high values (>5000 m/s) for Subunit 1B, but only in Hole 876A. Velocity data are sparse in Hole 876A and may not be representative of the entire unit. The data are, nevertheless, consistent with the higher density values, and the "well-cemented" lithology found in this hole. Two test cubes in Hole 876A represent Subunit 1B, whereas this subunit is unrepresented in the Hole 875C data. Most limestone samples from Subunits 1A and 1C in Hole 876A proved to be untestable as a result of the complete attenuation of the compressional wave signal by the coarse skeletal structure of the rock. Those tests that achieved a result did so with a poor signal. Compressional wave velocity anisotropy is high, most probably because of the bad signals (Table 11) in Holes 875C and 876A, which range from –0.17 to +0.15.

### Basalt

Geotechnical Unit 2 is represented by the alkalic basalt flows in the bottom of Holes 875C and 876A (Hole 875C, 126.0–133.0 mbsf; Hole 876A, 145.5–154.0 mbsf). These basalts are relatively unweathered compared with those from Holes 873 and 874 ("Igneous Petrology" section, this chapter). Dry-bulk density and grain density values in both holes range from 1.72 to 2.91 g/cm<sup>3</sup> and from 2.68 to 3.34 g/cm<sup>3</sup>, respectively; their mean values are 2.32 and 3.04 g/cm<sup>3</sup>, respectively.

## DOWNHOLE MEASUREMENTS AND SEISMIC STRATIGRAPHY

### Drilling Penetration Rates and Implications for Lithostratigraphy

Downhole logging runs were not performed in any of the holes at Sites 875 or 876 because of problems with hole stability, inadequate penetration, and/or time constraints. However, drilling penetration rates in Holes 875C and 876A, which penetrated through the carbonate platform to the uppermost volcanics, provide a proxy for relative lithology and cementation of the different facies (Figs. 24–25). At other sites on Wodejebato Guyot, vari-

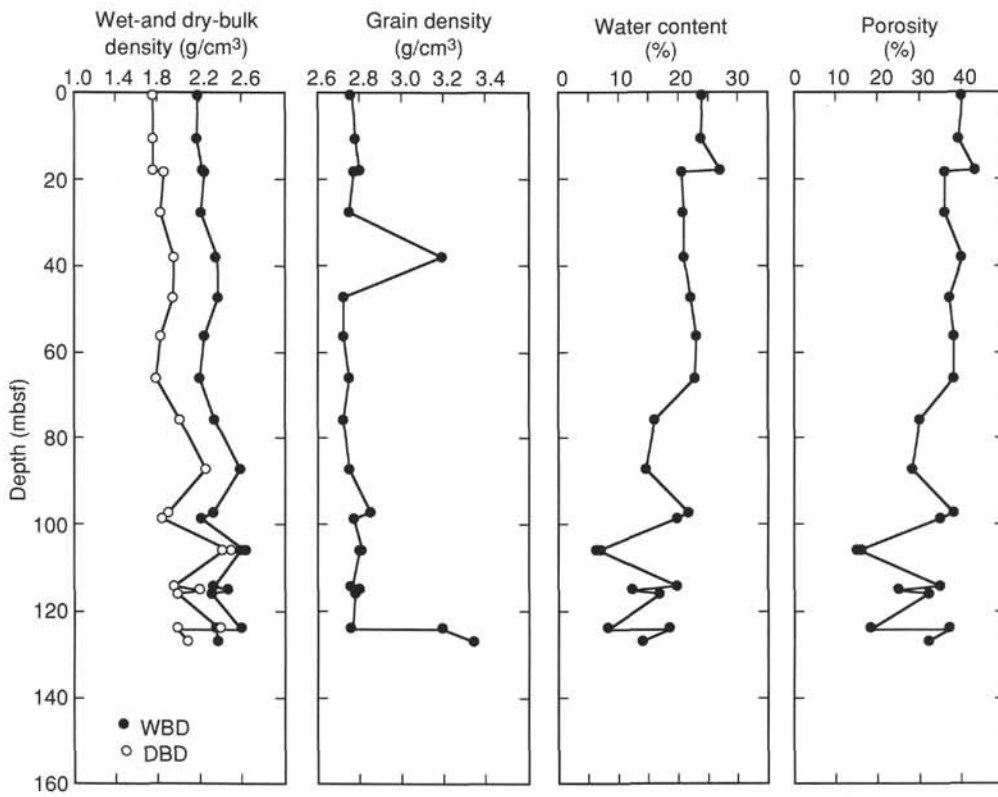


Figure 21. Measurements of index properties (wet- and dry-bulk density, grain density, water content, and porosity) vs. depth, Hole 875C.

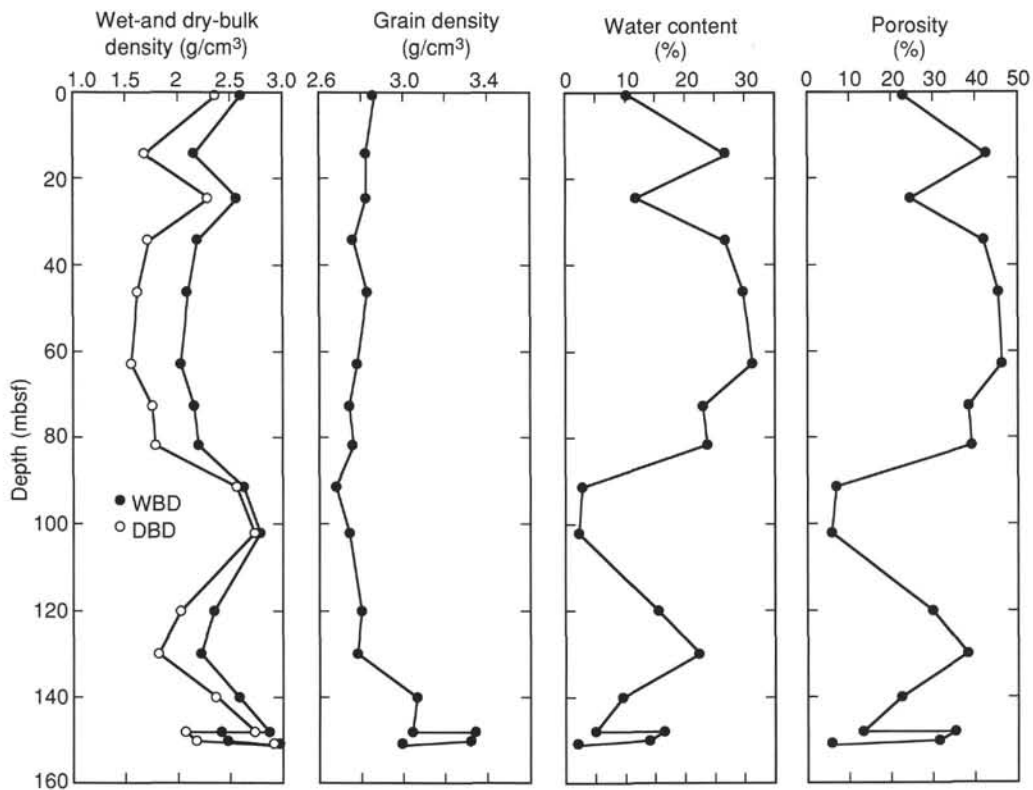


Figure 22. Measurements of index properties (wet- and dry-bulk density, grain density, water content, and porosity) vs. depth, Hole 876A.

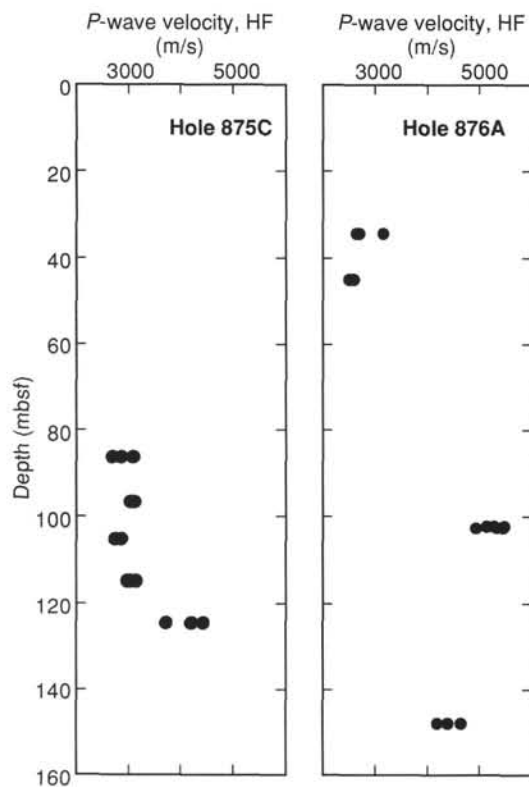


Figure 23. Hamilton Frame (HF) measurements of compressional wave velocity vs. depth, Holes 875C and 876A.

ations in penetration rates were observed to coincide with resistivity and density fluctuations and, therefore, may be related to porosity (e.g., “Site 873” chapter, Figs. 51–52; “Site 874” chapter, Fig. 35). Major changes in drilling rates can be used to assign boundaries between some major lithologic units and to define the contact with the hard basaltic basement.

Within Holes 875C and 876A on the outer perimeter ridge of Wodejebato Guyot, the pattern of downhole variations in drilling penetration rates are similar, thereby indicating a nearly identical succession of lithologic facies. In general, a thick series of loosely cemented grainstones contains a thin interval of harder lithology at about 100 to 110 mbsf. These observations agree with the lithostratigraphy at these two sites (see “Lithostratigraphy” section, this chapter).

### Upper Skeletal Grainstone Facies (Lithologic Subunit IIA)

Drilling penetration rates in the upper two-thirds of the carbonate platform (upper 110 m in Hole 875C, upper 95 m in Hole 876A) were very rapid, ranging from 0.5 to 1.0 m (2 to 1 min/m), with no significant fluctuations (Figs. 24–25). This interval corresponds to Lithologic Subunit IIA (Core 144-875C-1M to the middle of Core 144-875C-12M, and Core 144-876A-1R to the top of Core 144-876A-10R), which is composed of coarse-grained, poorly consolidated, skeletal grainstone at each site. The uppermost core in each hole (Cores 144-875C-1M and 144-876A-1R) required longer to drill, partially the result of the dense manganese crust (Lithologic Unit I) at the sediment surface, and also because of a blockage in the drill bit through this interval in Hole 875C. In both holes, the drill pipe was lowered into a shallow pocket of white ooze overlying the hardened top of the carbonate platform;

Table 11. Hamilton Frame measurements of compressional wave velocity, Holes 875C and 876A.

Core, section, interval (cm)	Depth (mbsf)	Distance (mm)	Axes of measurements	Traveltime (μs)	Corrected traveltime (μs)	Measured velocity (m/s)	Velocity anisotropy index
144-875C-							
10M-1, 50–52	85.50	20.85	a	10.91	7.91	2635.90	
10M-1, 50–52	85.50	21.54	b	10.67	7.67	2808.34	
10M-1, 50–52	85.50	21.93	c	10.22	7.22	3039.50	-0.11
11M-1, 121–123	95.91	22.36	a	10.56	7.56	2959.63	
11M-1, 121–123	95.91	21.39	b	10.11	7.11	3010.56	
11M-1, 121–123	95.91	21.37	c	10.05	7.05	3033.36	-0.02
12M-1, 30–32	104.60	21.40	b	10.63	7.63	2806.56	
12M-1, 30–32	104.60	21.39	c	11.00	8.00	2673.75	0.05
13M-1, 24–26	114.14	20.75	a	10.01	7.01	2960.06	
13M-1, 24–26	114.14	21.14	b	9.88	6.88	3072.67	
13M-1, 24–26	114.14	21.16	c	10.27	7.27	2910.59	0.04
14M-1, 15–17	123.75	20.81	a	8.02	5.02	4149.55	
14M-1, 15–17	123.75	21.19	b	7.86	4.86	4360.08	
14M-1, 15–17	123.75	21.30	c	8.83	5.83	3656.65	0.15
144-876A-							
4R-1, 102–104	34.32	22.85	a	11.51	8.51	2686.66	
4R-1, 102–104	34.32	21.22	b	11.11	8.11	2616.52	
4R-1, 102–104	34.32	22.96	c	10.32	7.32	3138.76	-0.17
5R-2, 50–52	45.00	22.01	a	11.87	8.87	2481.40	
5R-2, 50–52	45.00	21.01	b	11.36	8.36	2514.66	
5R-2, 50–52	45.00	21.21	c	11.27	8.27	2564.69	-0.03
11R-1, 115–117	101.95	21.52	a	6.96	3.96	5441.21	
11R-1, 115–117	101.95	20.30	b	6.88	3.88	5238.71	
11R-1, 115–117	101.95	17.69	c	6.46	3.46	5120.12	0.04
11R-2, 23–25	102.43	14.66	a	5.77	2.77	5301.99	
11R-2, 23–25	102.43	21.64	b	6.99	3.99	5430.36	
11R-2, 23–25	102.43	22.00	c	7.49	4.49	4905.24	0.09
16R-1, 6–8	147.86	20.32	a	7.87	4.87	4172.49	
16R-1, 6–8	147.86	21.70	b	7.98	4.98	4361.81	
16R-1, 6–8	147.86	21.49	c	7.65	4.65	4621.51	-0.08

Notes: a = direction perpendicular to split core plane, b = direction transverse to split core plane, and c = core axis; all axes orthogonal.

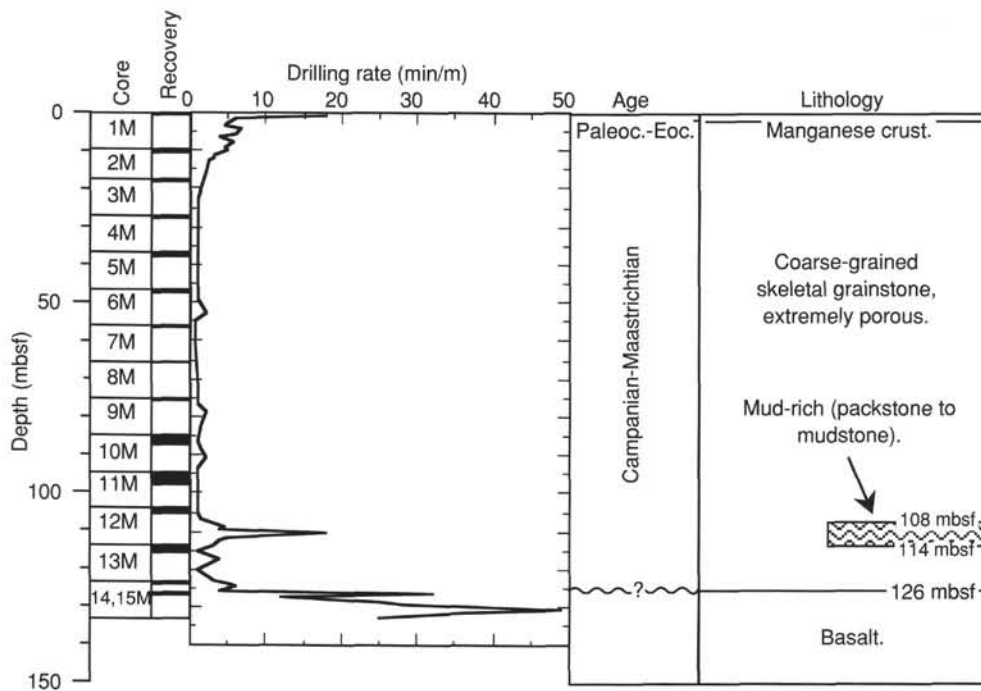


Figure 24. Stratigraphy of Hole 875C from drilling rates compared to cored intervals, lithostratigraphy, and biostratigraphic ages within Hole 875C. Drilling rates are plotted as the minutes required to penetrate 1 m, which yields a visual display comparable to the resistivity or density logs.

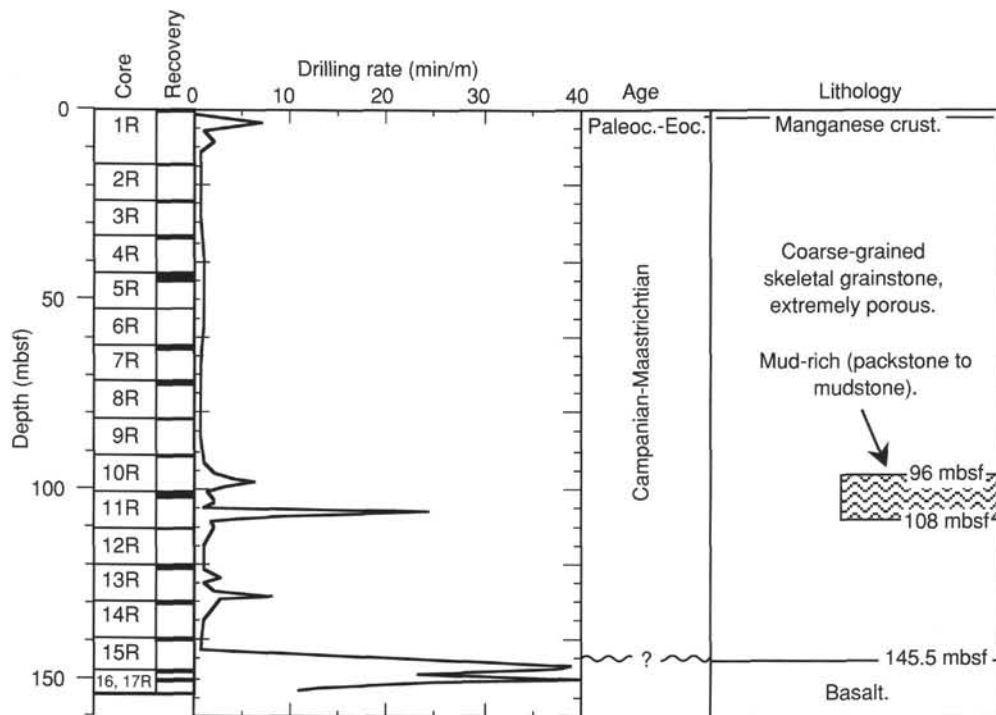


Figure 25. Stratigraphy of Hole 876A from drilling rates compared to cored intervals, lithostratigraphy, and biostratigraphic ages within Hole 876A. Drilling rates are as in Figure 23.

this pelagic ooze, which did not display any resistance to the lowered drill pipe, was not recovered, however.

### Well-cemented Skeletal Packstone Facies (Lithologic Subunit IIB)

The upper, loosely cemented grainstone (Subunit IIA) is underlain by an interval of harder lithology composed of burrowed, lime-mud-rich limestone. This facies has slightly different characteristics at each of the two sites (Figs. 24–25), but it is similar in its relative thickness, fossil assemblages, and relationship to adjacent facies. This suggests that the relatively well-cemented interval comprising Subunit IIB may represent a condensed sedimentary section and/or a period of quieter depositional conditions (see "Lithostratigraphy" section, this chapter).

In Hole 875C, penetration rates from 108 through 114 mbsf (corresponding to the lower half of Core 144-875C-12M) were less than 0.3 m/min, with a minimum of 0.06 m/min at 110–112 mbsf. This 6-m-thick interval corresponds to the recovery of foraminifer skeletal packstone containing intraclasts and of gastropod-bearing mudstone.

In Hole 876A, penetration rates from 96 through 106 mbsf (corresponding to Cores 144-876A-10R and uppermost -11R) were generally less than 0.5 m/min. This 10-m-thick interval corresponds to the recovery of a fine-grained facies of stromatoporoid-bearing algal-skeletal wackestone and packstone. In the underlying 2 m (106–108 mbsf), slower drilling penetration rates of less than 0.2 m/min probably correspond to a well-cemented skeletal packstone to wackestone recovered in the lower part of Core 144-876A-11R.

### Lower Skeletal Grainstone Facies (Lithologic Subunit IIC)

The lower portion of the carbonate platform at each of the two sites is a porous grainstone facies (Cores 144-875C-13M to -14M, and lower Core 144-876A-11R to uppermost -15R, respectively), which has similar lithologic characteristics and drilling penetration rates (0.5–1.0 m/min) to the upper skeletal grainstone of Lithologic Subunit IIA (Figs. 24–25).

In Hole 875A, an interval of slightly slower drilling penetration rates at 117–118 mbsf may correspond to the horizons with mudstone intraclasts observed within the middle of Core 144-875C-13M; slower drilling penetration rates at 123 and 126 mbsf may represent the moderately cemented skeletal grainstone overlying basaltic basement. In Hole 876A, an interval of slower penetration at 128 mbsf may be caused by the increased cementation of the lowermost algal foraminifer grainstone observed in Interval 144-876A-13R-1, 40–119 cm.

### Volcanic Edifice (Lithologic Unit III)

The top of the hard basaltic basement is clearly marked by a greatly reduced penetration rate (Figs. 24–25). In Hole 875C, contact is made with a very hard lithology at 126 mbsf. Therefore, we place the base of the carbonate platform in Hole 875C at 126 mbsf (or 1535 mbsl). In Hole 876A, the contact with the very hard lithology is at 145.5 mbsf (or 1545 mbsl, only 10 m lower than in Hole 875C).

Within the basaltic basement in each hole is a horizon of harder basalt situated about 4 m below the top of the volcanic facies. In Hole 875C, this hard horizon is at 130–131 mbsf; in Hole 876A, it is at 150 mbsf. A similar horizon of hard basalt, situated about 4 m below the top of the volcanic facies, is also apparent in the drilling records from nearby Hole 874B on the inner perimeter ridge. Low recovery prevented a determination of the basalt lithology that is responsible for producing these relatively hard

layers at a consistent depth within the uppermost volcanic edifice at the various sites.

### Seismic Stratigraphy Interpretation

Single-channel seismic profiles were obtained while crossing Sites 875 and 876, using a 200-in.<sup>3</sup> water gun as a sound source. These data were recorded on a Masscomp computer, refiltered and displayed, but were found to be inferior to a multichannel seismic record collected during a previous survey across the location of Sites 874 and 875 with two 80-in.<sup>3</sup> water guns shot to a six-channel seismic streamer. These multichannel data were processed up through migration and are displayed in Figure 26. Comparison with the coring results suggests some correlations to the recovered lithologic section.

The seafloor at Hole 875C is a "hardground" surface of probable latest Maastrichtian through middle Eocene age. This surface is marked by a hard, opaque seafloor reflector on both the 3.5-kHz and seismic reflection records (Fig. 26). Below this hard reflector is a seismic unit that extends from the seafloor at 1.91 to 2.01 s two-way traveltime (TWT), which we correlate with the entire limestone section at Hole 875C. Thus, the reflector at 2.01 s TWT does correlate with the top of basement at 126 mbsf. The average formation velocity of the limestone section has been calculated from its 126-m-thick and 1.00-s-TWT interval to be 2.5 km/s. This average velocity is in accord with the formation velocities measured in similar formations at other Leg 144 sites.

Drilling in Hole 875C ended at 133 mbsf. No coherent seismic reflectors are seen below the basement reflector at 2.01 s TWT.

The above correlations and formation velocities are reasonably confident statements of in-situ conditions at Hole 875C. As such, they can be used with regional seismic surveys to construct a seismic stratigraphic map of the entire Wodejebato Guyot platform.

The seismic reflection profiles across the Site 876–877 transect were unsuitable for use in an unambiguous identification of basement reflector; therefore, no seismic stratigraphy interpretations were attempted.

In summary, the drilled and seismic stratigraphy sections at Sites 875 and 876 on Wodejebato Guyot may be divided into three main parts:

1. A manganese crust overlying the carbonate platform, with an apparent hiatus in sedimentation from latest Cretaceous to the present.
2. A carbonate platform, 126 m thick in Hole 875C and 145.5 m thick in Hole 876A, that consists primarily of loosely consolidated, coarse-grained skeletal grainstone. A harder, 6- to 12-m-thick, burrowed, mud-rich facies can be seen at about 110 mbsf at each site (108–114 mbsf in Hole 875C, and 96–108 mbsf in Hole 876A).
3. A lower volcanic edifice having a weathered upper surface. The top of the volcanic edifice is at 126 mbsf in Hole 875C and at 145.5 mbsf in Hole 876A.

### SUMMARY AND CONCLUSIONS

Holes 875C and 876A both ended in alkalic basalt flows. All the lavas recovered at both sites, including the flow-top breccia, share the dominant mineralogical characteristics of all the flows from Wodejebato Guyot. The mineralogy of the flows is consistent with a slight to moderate degree of undersaturation, similar to the alkalic cap stage of Hawaiian volcanism. These flows most likely represent a subaerial sequence; however, both outer perimeter ridge sites do not record significant weathering intervals before the onset of marine conditions. The uppermost basalt at

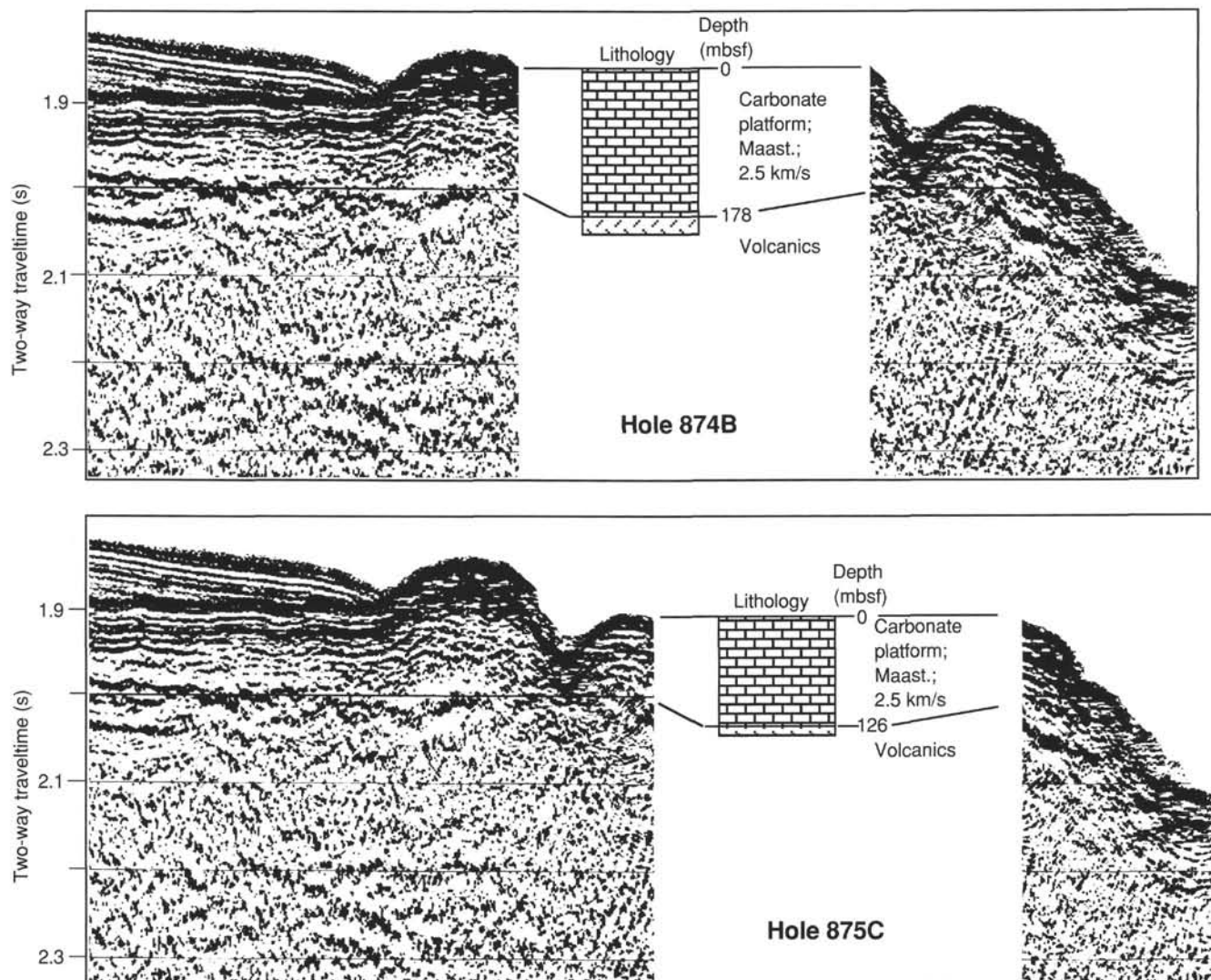


Figure 26. Lithostratigraphic correlations to the seismic stratigraphy sections crossing Holes 874B and 875C. Major reflectors correspond to stratigraphic breaks in deposition or to major facies changes. The position of the top of the volcanics in meters is based on measurements of drilling rates.

Site 875 was affected by reducing conditions, as inferred by the presence of pyrite at the top of the youngest unit, whereas some oxidative weathering affected the uppermost basalt at Site 876.

In possibly the late Campanian or early Maastrichtian, a transgression of the sea over the basalt occurred with moderately high-energy conditions, as demonstrated by the presence of reworked basalt pebbles at the base of the skeletal sands at both sites. The poorly cemented sand encountered at Sites 875 and 876 contains abundant fragments of Late Cretaceous organisms, with larger foraminifers as a dominant constituent. Planktonic foraminifers occur throughout, except near the top of the sequence. The sands are well winnowed, moderately sorted, and abraded. No blocks of boundstone or other reef lithology were encountered. These characteristics suggest that the sands underwent considerable reworking before deposition. The reworking of these sands, in conjunction with the persistent occurrence of planktonic foraminifers, suggests that the depositional setting for these units was a fore-reef apron, seaward of the reef tract. The reef tract setting is thought to be located at the inner perimeter ridge, which was drilled at Sites 874 and 877.

A shoaling episode interrupted this monotonous sedimentation of reworked sands. This shoaling is represented by cemented

skeletal packstone, with lenses of muddier wackestone interbedded in the poorly cemented grainstone, and a layer of mudstone. Although the major skeletal components of the packstone and wackestone remain nearly identical to those from the overlying and underlying grainstones, the mudstone contains only small gastropod molds, ostracodes, and small benthic foraminifers. This assemblage indicates a restricted environment. The absence of planktonic foraminifers in the uppermost part of the grainstone sequence possibly indicates a shallow-water environment until the end of sand deposition in the Maastrichtian.

Exposure of this shoal may have been extensive; evidence for exposure is the occurrence of cavities at least 30 cm deep, and the infiltration of pelagic ooze at least 70 cm deep into the sands to become the matrix of the grainstone. During the VIT survey at these outer perimeter ridge sites, about 1 m of relief was noted in unconnected depressions in the manganese-encrusted surface of the limestone. This suggests that a microkarstic surface potentially formed between the middle to late(?) Maastrichtian and the late Paleocene, before submergence of the platform into the pelagic realm. The overall lack of pelagic ooze, and the presence of manganese-encrusted, phosphatized lithoclasts of varying origins and ages overlying the cavities containing pelagic infilling, sug-

gest that Sites 875 and 876 were, and still are, a location of prevailing nondeposition of sediment.

#### REFERENCES\*

- Bergersen, D.D., in press. Geology and geomorphology of Wodejebato (Sylvania) Guyot, Marshall Islands. In Pringle, M., and Sliter, W. (Eds.), *The Mesozoic Pacific*. Am. Geophys. Union.
- Enos, P., and Sawatsky, L.H., 1981. Pore networks in Holocene carbonate sediments. *J. Sediment. Petrol.*, 51:961-985.
- Folk, R.L., 1967. Sand cays of Alacran Reef, Yucatan, Mexico: morphology. *J. Geol.*, 75:412-437.
- Folk, R.L., and Robles, R., 1964. Carbonate sands of Isla Perez, Alacran reef complex, Yucatan. *J. Geol.*, 72:255-292.
- McKee, E.D., Chronic, J., and Leopold, E.B., 1959. Sedimentary belts in lagoon of Kapingamarangi Atoll. *AAPG Bull.*, 43:501-526.
- Perch-Nielsen, K., 1985. Cenozoic calcareous nannofossils. In Bolli, H.M., Saunders, J.B., and Perch-Nielsen, K. (Eds.), *Plankton Stratigraphy*: Cambridge (Cambridge Univ. Press), 427-554.
- Premoli Silva, I., and Brusa, C., 1981. Shallow-water skeletal debris and larger foraminifers from Deep Sea Drilling Project Site 462, Nauru Basin, western equatorial Pacific. In Larson, R.L., Schlanger, S.O., et al., *Init. Repts. DSDP*, 61: Washington (U.S. Govt. Printing Office), 439-473.

\* Abbreviations for names of organizations and publication titles in ODP reference lists follow the style given in *Chemical Abstracts Service Source Index* (publish-

144IR-108

**NOTE: For all sites drilled, core-description forms ("barrel sheets") and core photographs can be found in Section 3, beginning on page 453. Forms containing smear-slide data can be found in Section 4, beginning on page 1017. Thin-section data are given in Section 5, beginning on page 1037.**